Available online at www.sciencedirect.com
ScienceDirect
Comput. Methods Appl. Mech. Engrg. 365 (2020) 112957
Computer methods in applied mechanics and engineering
www.elsevier.com/locate/cma

A projection based variational multiscale method for a fluid–fluid interaction problem

Mustafa Aggul[a], Fatma G. Eroglu[b], Songül Kaya[c], Alexander E. Labovsky[d,*]

[a] Department of Mathematics, Hacettepe University, Ankara 06800, Turkey
[b] Department of Mathematics, Faculty of Science, Bartın University, Bartın 74110, Turkey
[c] Department of Mathematics, Middle East Technical University, Ankara 06800, Turkey
[d] Department of Mathematical Sciences, Michigan Technological University, Houghton, MI 49931, USA

Received 23 October 2019; received in revised form 19 February 2020; accepted 20 February 2020
Available online 25 March 2020

Abstract

The proposed method aims to approximate a solution of a fluid–fluid interaction problem in case of low viscosities. The nonlinear interface condition on the joint boundary allows for this problem to be viewed as a simplified version of the atmosphere–ocean coupling. Thus, the proposed method should be viewed as potentially applicable to air–sea coupled flows in turbulent regime. The method consists of two key ingredients. The geometric averaging approach is used for efficient and stable decoupling of the problem, which would allow for the usage of preexisting codes for the air and sea domain separately, as "black boxes". This is combined with the variational multiscale stabilization technique for treating flows at high Reynolds numbers. We prove the stability and accuracy of the method, and provide several numerical tests to assess both the quantitative and qualitative features of the computed solution.

Keywords: Fluid–fluid interaction; Variational multiscale methods; Partitioned methods

1. Introduction

The study of solving coupled Navier–Stokes equations with special interface conditions is of considerable interest, for instance in the simulation of atmosphere–ocean (AO) interaction or two layers of a stratified fluid. In this paper, we investigate a low-viscosity fluid–fluid interaction problem, aiming at modeling AO flow in a turbulent regime.

Consider the d-dimensional ($d = 2, 3$) polygonal or polyhedral domain Ω in space that consists of two subdomains Ω_1 and Ω_2, coupled across an interface I, for times $t \in [0, T]$. Coupling problem is: given $\nu_i > 0$, $f_i : [0, T] \to H^1(\Omega_i)^d$, $u_i(0) \in H^1(\Omega_i)^d$ and $\kappa \in \mathbb{R}$, find (for $i = 1, 2$) $u_i : \Omega_i \times [0, T] \to \mathbb{R}^d$ and $p_i : \Omega_i \times [0, T] \to \mathbb{R}$ satisfying (for $0 < t \leq T$)

$$\partial_t u_i - \nu_i \Delta u_i + u_i \cdot \nabla u_i + \nabla p_i = f_i \quad \text{in } \Omega_i, \tag{1.1}$$

$$-\nu_i \hat{n}_i \cdot \nabla u_i \cdot \tau = \kappa |u_i - u_j|(u_i - u_j) \cdot \tau \quad \text{on } I \text{ for } i, j = 1, 2, \ i \neq j\,, \tag{1.2}$$

* Corresponding author.
E-mail addresses: mustafaaggul@hacettepe.edu.tr (M. Aggul), fguler@bartin.edu.tr (F.G. Eroglu), smerdan@metu.edu.tr (S. Kaya), aelabovs@mtu.edu (A.E. Labovsky).

https://doi.org/10.1016/j.cma.2020.112957
0045-7825/

$$u_i \cdot \hat{n}_i = 0 \qquad \text{on } I \text{ for } i, j = 1, 2, \tag{1.3}$$

$$\nabla \cdot u_i = 0 \qquad \text{in } \Omega_i, \tag{1.4}$$

$$u_i(x, 0) = u_i^0(x) \qquad \text{in } \Omega_i, \tag{1.5}$$

$$u_i = 0 \qquad \text{on } \Gamma_i = \partial\Omega_i \setminus I, \tag{1.6}$$

where $|\cdot|$ represents the Euclidean norm and the vectors $\hat{n}_i$ are the unit normals on $\partial\Omega_i$, and τ is any vector such that $\tau \cdot \hat{n}_i = 0$. Here u_i, and p_i denote the unknown velocity fields and pressure. The parameters are ν_i kinematic viscosities, f_i the body forcing on the velocity, κ the friction parameter (frictional drag force is assumed to be proportional to the square of the jump of the velocities across the interface).

Numerical methods for solving this type of coupled problems in laminar flow regime have been investigated [1–4]. In [2], IMEX and geometric averaging (GA) time stepping methods have been proposed (and further developed in [4]) for the Navier–Stokes equations with nonlinear interface condition.

The study of fluid–fluid interaction has received considerable interest in the last thirty years, starting with the seminal paper of Lions, Temam and Wang, [5,6], on the analysis of full equations for AO flow. Today, many models exist and an abundance of software code is available for climate models (both global and regional), hurricane propagation, coastal weather prediction, etc. see, e.g., [7–9] and references therein. The reasoning behind most of these models is as follows: the boundary condition on the joint AO interface must be chosen in such a way, that fluxes of conserved quantities are allowed to pass from one domain to the other. In particular, the nonlinear interface condition (1.2), together with (1.3) ensures that the energy is being passed between the two domains in the model above, with the global energy still being conserved.

The AO coupling problem (as well as its modest version, the fluid–fluid interaction with nonlinear coupling, considered in this report) provides many challenges. In addition to the usual issues one has to overcome when solving the Navier–Stokes equations, the AO models should allow to use different spacial and temporal scales for the atmosphere and ocean domains, as the energy in the atmosphere remains significant at smaller time scales and larger spatial scales, than the energy of the ocean. In order to do so, as well as make use of the existing codes written separately for the fluid flows in the air or the ocean domains, one needs to create partitioned methods, that allow for a stable and accurate decoupling of the AO system.

The literature on numerical analysis of time-dependent coupling problem (1.1)–(1.6) is somewhat scarce; some approaches to creating a stable, accurate, computationally attractive decoupling method can be found in [1–4,10,11]. The methods in [4,11] provide second order accuracy in temporal discretization. However, the authors could not find any reports on methods for approximating the solution of (1.1)–(1.6) in a turbulent regime. This problem is magnified over the usual issues in turbulence modeling, because of several extra obstacles: the size of the problem, the necessity to treat the atmosphere and ocean codes as "black boxes" — therefore utilizing one of only a few existing decoupling methods; and, finally, the lack of benchmark problems for turbulent AO coupling. We propose to start working in this direction by using a stabilization technique for low-viscosity problem (1.1)–(1.6).

Various stabilizations have proven to be essential computational tools for the numerical simulations. The general idea of two level stabilization is pioneered by Marion and Xu in [12] and the analysis for Navier–Stokes is presented in seminal papers [13,14]. This idea has been strongly connected with variational multiscale (VMS) methods introduced in [15,16]. VMS methods have proven to be an accurate and systematic approach to the numerical simulation of multiphysics flows and different realizations of VMS in the literature exist, e.g., see [17–20]. In particular, we consider a projection-based VMS in this paper which has been proposed in [21]. According to VMS concept, global stabilization is introduced in all scales, then removes the effective stabilization on the large scales of the solution. In this way, stabilization is effective only on the smallest scales, where the non-physical oscillations occur. For more details, we refer the reader to [19,20]. We also refer to [22] for the derivation of the different VMS methods for turbulent flow simulations.

Due to the success of VMS method, there is a natural desire to introduce this accurate and systematic approach to the simulation of fluid–fluid interaction. We consider an extension of VMS method with GA of the nonlinear interface condition. As first contribution of this paper, we first show the conservation of GA-VMS method's discrete kinetic energy, frequently evaluated quantity of interest in AO flow simulations along with stability and long-time stability properties of GA-VMS method. We show both stability bounds are unconditional, i.e., without any restriction on time step size. Secondly, we provide a precise analysis of the stability, convergence and accuracy of the

GA-VMS method. Lastly, we present numerical studies in case of different viscosities compared with monolithically coupled algorithms.

The paper is organized as follows. The GA-VMS method for solving (1.1)–(1.6) in the case of high Reynolds number(s) is presented in Section 2, along with a short discussion on an alternative formulation of the method. After mathematical preliminaries are introduced in Section 3, a complete numerical analysis is then done on the proposed method in Section 4. Finally, Section 5 provides the numerical tests that validate the theoretical findings, and conclusions are given in Section 6.

2. GA-VMS method for fluid–fluid interaction problem

In this paper, standard notations of Lebesgue and Sobolev spaces are used. Let each subdomain $\Omega_i \subset \mathbb{R}^d, i = 1, 2, d = 2, 3$ be a bounded domain. The L^2 space is equipped with the inner product, $(\cdot,\cdot)_{\Omega_i}$ and the norm $\|\cdot\|_{\Omega_i}$. In particular, the norm $L^3(I)$ at the interface will be denoted by $\|\cdot\|_I$. In each subdomain, the spaces $H^k(\Omega_i)^d$ and $L^p(0, T; H^k(\Omega_i))$ are equipped with the norms $\|\cdot\|_{k,\Omega_i}$ and $\|\cdot\|_{L^p(0,T;H^k(\Omega_i))}$, respectively. The norm of the dual space of $H^{-1}(\Omega_i)$ of $H_0^1(\Omega_i)$ and the semi-norm of H^k, for $1 \le k < \infty$ are denoted by $\|\cdot\|_{-1,\Omega_i}$ and $|\cdot|_k$, respectively.

For the weak formulation of problem (1.1)–(1.6), we use the function spaces for $i = 1, 2$

$$X_i := \{v \in (L^2(\Omega_i))^d : \nabla v \in L^2(\Omega_i)^{d\times d},\ v = 0 \text{ on } \partial\Omega_i\backslash I,\quad v\cdot\hat{n}_i = 0 \text{ on } I\},$$
$$Q_i = L_0^2(\Omega_i) := \{q \in L^2(\Omega_i) : \int_{\Omega_i} q\, dx = 0\}.$$

Herein, define $X = X_1 \times X_2$, $Q = Q_1 \times Q_2$ and $L^2(\Omega) = L^2(\Omega_1)\times L^2(\Omega_2)$. For $u_i \in X_i$ and $q_i \in Q_i$, we denote $\mathbf{u} = (u_1, u_2)$ and $\mathbf{q} = (q_1, q_2)$, respectively. For $\mathbf{u}, \mathbf{v} \in X$, the L^2 inner product and induced norm are denoted by $(\mathbf{u}, \mathbf{v})$ and $\|\mathbf{u}\| = \sqrt{(\mathbf{u}, \mathbf{u})}$. In a similar manner, the H^1 inner product and induced norm are denoted by $(\mathbf{u}, \mathbf{v})_X$ and $\|\mathbf{u}\|_X = \sqrt{(\mathbf{u}, \mathbf{u})_X}$, respectively.

Using these function spaces, the weak formulation of (1.1)–(1.6) is as follows: Find $(u_i, p_i) \in (X_i, Q_i)$ for $i, j = 1, 2,\ i \ne j$ such that for all $(v_i, q_i) \in (X_i, Q_i)$.

$$(\partial_t u_i, v_i)_{\Omega_i} + \nu_i(\nabla u_i, \nabla v_i)_{\Omega_i} + c_i(u_i; u_i, v_i) - (p_i, \nabla\cdot v_i)_{\Omega_i} + (\nabla\cdot u_i, q_i)_{\Omega_i}$$
$$+\kappa\int_I |u_i - u_j|(u_i - u_j)v_i ds = (f_i, v_i)_{\Omega_i}. \tag{2.1}$$

Here and in the rest of the paper, $c_i(\cdot;\cdot,\cdot)$ denotes the usual, explicitly skew symmetrized trilinear form

$$c_i(u; v, w) = \frac{1}{2}(u\cdot\nabla v, w)_{\Omega_i} - \frac{1}{2}(u\cdot\nabla w, v)_{\Omega_i} \tag{2.2}$$

for functions $u, v, w \in X_i$, $i = 1, 2$ on Ω_i. Notice the well known property

$$c_i(u; v, w) = -c_i(u; w, v)$$

for all $u, v, w \in X_i$ such that in particular $c_i(u; v, v) = 0$ for all $u, v \in X_i$.

The standard monolithic weak formulation of (1.1)–(1.6) is obtained by summing (2.1) over for $i, j = 1, 2,\ i \ne j$ and is to find $(\mathbf{u}, p) \in (X, Q)$ such that for all $(\mathbf{v}, \mathbf{q}) \in (X, Q)$

$$(\partial_t\mathbf{u}, \mathbf{v}) + \nu(\nabla\mathbf{u}, \nabla\mathbf{v}) + c(\mathbf{u}; \mathbf{u}, \mathbf{v}) - (\mathbf{p}, \nabla\cdot\mathbf{v}) + (\nabla\cdot\mathbf{u}, \mathbf{q}) + \kappa\int_I |[\mathbf{u}]|[\mathbf{u}][\mathbf{v}]ds = (\mathbf{f}, \mathbf{v}), \tag{2.3}$$

where $[\cdot]$ denotes the jump across the interface I and $\mathbf{f} = f_i$, $\nu = \nu_i$ on Ω_i.

For finite element discretization, let T_i^h and T_i^H be admissible triangulations of Ω_i, where T_i^h refers to fine mesh and T_i^H denotes the coarse mesh, i.e. $H \ge h$. Let $(X_i^h, Q_i^h) \subset (X_i, Q_i)$ be conforming finite element spaces satisfying the so-called discrete inf–sup condition [23,24]. In our tests, we have used the velocity-pressure pairs of spaces (P_k, P_{k-1}), $k \ge 2$. Let V_i^h be the space of the discretely divergence-free functions

$$V_i^h = \{v_{h,i} \in X_i^h : (q_{h,i}, \nabla\cdot v_{h,i})_{\Omega_i} = 0,\ for\ all\ q_{h,i} \in Q_i^h\}, \tag{2.4}$$

which is a closed subspace of X_i^h. The dual space of V_i^h is given by V_i^{h*} with norm $\|\cdot\|_{V_i^{h*}}$. We also need to introduce the space

$$L^\infty(\mathbb{R}^+, V_i^{h*}) = \{f_i : \Omega_i^d \times \mathbb{R}^+ \to \mathbb{R}, \exists M < \infty\ with\ \|f_i(t)\|_{V_i^{h*}} < M\, a.e.\, t > 0\} \tag{2.5}$$

To solve two decoupled systems (atmosphere and ocean separately) through GA on the interface with the projection-based VMS formulation, for each subdomain let

$$L_i^H \subset L : (L^2(\Omega))^{d\times d}$$

be a continuous finite element space of functions defined on Ω_i representing a coarse or large scale space and let $\nu_{T,i}$ be eddy viscosity term assumed herein a non-negative function depending on the mesh size h.

We now present the projection-based VMS discretization of (2.1) by using the Euler method in time. For this purpose, consider a partition $0 = t_0 < t_1 < \cdots < t_{M+1} = T$ of the time interval $[0, T]$ and define $\Delta t = T/(M+1)$, $t_n = n\Delta t$. GA-VMS formulation applied to the problem (2.1) reads as follows: Given $u_{h,i}^0, u_{h,i}^1 \in X_i^h$, find $(u_{h,i}^{n+1}, p_{h,i}^{n+1}, \mathbb{G}_i^{\mathbb{H},n+1}) \in (X_i^h, Q_i^h, L_i^H)$, $n = 1, \ldots, M$, satisfying

$$\begin{aligned}
&(\frac{u_{h,i}^{n+1} - u_{h,i}^n}{\Delta t}, v_{h,i})_{\Omega_i} + (\nu_i + \nu_{T,i})(\nabla u_{h,i}^{n+1}, \nabla v_{h,i})_{\Omega_i} + c_i(u_{h,i}^{n+1}; u_{h,i}^{n+1}, v_{h,i}) - (p_{h,i}^{n+1}, \nabla\cdot v_{h,i})_{\Omega_i}\\
&+ (\nabla\cdot u_{h,i}^{n+1}, q_{h,i})_{\Omega_i} + \kappa\int_I |[\mathbf{u}_h^n]| u_{h,i}^{n+1} v_{h,i} ds - \kappa\int_I u_{h,j}^n |[\mathbf{u}_h^n]|^{1/2} |[\mathbf{u}_h^{n-1}]|^{1/2} v_{h,i} ds\\
&= (f_i^{n+1}, v_{h,i})_{\Omega_i} + \nu_{T,i}(\mathbb{G}_i^{\mathbb{H},n}, \nabla v_{h,i})_{\Omega_i} \qquad (2.6)\\
&(\mathbb{G}_i^{\mathbb{H},n} - \nabla u_{h,i}^n, \mathbb{L}_i^H)_{\Omega_i} = 0, \qquad (2.7)
\end{aligned}$$

for all $(v_{h,i}, q_{h,i}, \mathbb{L}_i^H) \in (X_i^h, Q_i^h, L_i^H)$.

Remark 2.1. In (2.7), the tensor $\mathbb{G}_i^{\mathbb{H},n}$ represents the large scales of $\nabla u_{h,i}$, defined by L^2-projection of $\nabla u_{h,i}^n$ on Ω_i into the large scale space L_i^H (see Definition 3.1). Hence, the difference $\mathbb{G}_i^{\mathbb{H},n} - \nabla u_{h,i}^n$ represents the resolved small scales. This way, the GA-VMS method (2.6)–(2.7) introduces the additional viscous term into the momentum equation acting only on the resolved small scales. We note that the L^2- projection terms for $\mathbb{G}_i^{\mathbb{H},n}$ can be discretized implicitly or explicitly in time. We will consider here the computationally attractive explicit discretization, and refer the reader to [20,25] for further discussions on explicit vs. implicit discretizations of $\mathbb{G}_i^{\mathbb{H},n}$.

In GA-VMS formulation of (2.6)–(2.7), the large scale spaces L_i^H and $\nu_{T,i}$ parameters must be chosen suitably. In [26], it was concluded that the choices of L_i^H have a large impact on the results. The large scale spaces have to be in some sense a coarse finite element space. Mainly, there are two approaches. The first approach is to define L_i^H using lower order finite element spaces on the same mesh, provided that finite element spaces (X_i^h, Q_i^h) are high enough order [20]. Second approach is to define L_i^H on a coarser grid, $H > h$, see, e.g., [19]. Herein, we will use the first approach, which is the most common choice in geophysical problems because of the very large scales of the problems studied. Thus, we choose L_i^H to be piecewise polynomials of degree $k-1$.

In general, VMS approach will treat the diffusion differently in each subdomain. For instance, one can model a turbulent atmospheric flow over a transitional or even laminar ocean flow; in that case, the choice $\nu_{T,1} = h$, $\nu_{T,2} = 0$ could be warranted. However, in order to address the most complicated case of both flows being turbulent, but also trying to minimize the number of parameters in the method, in our numerical experiments we choose $\nu_{T,i} = h$ in each subdomain (typical for various artificial viscosity-type models); different optimal parameter choices of eddy viscosity parameter require further investigations. In addition, we note that while the larger choice of the coarse mesh size H provides more efficient projections into large scale spaces L_i^H and reduces storage, the accuracy of the solutions decreases. For $k = 2$, the typical choice is $H = O(h^{1/2})$ for the projection-based VMS. This choice is obtained from balancing terms in the convergence analysis. In our numerical studies, we will use single mesh, that is $H = h$. With the space L_i^H consisting of piecewise polynomials of degree $k-1$, this creates a good balance between accuracy and required computational resources; see [20] for a similar discussion on the choice of L^H spaces.

It also has to be noted that while the projection steps between two time marching add extra computations beyond GA, these computations do not add extra time for computations and even increases the efficiency of the linear solvers, and hence decreases computational time, see Section 6. In addition, they do not require too much extra memory since only the projection of already-stored solutions from previous time level is taken on a space which has relatively much less degrees of freedom comparing to that of velocity spaces. Since the corresponding system matrix for the projection is symmetric and positive definite, it allows the usage of efficient iterative solvers such as conjugate gradients. Finally, we note that there are several possible realizations of VMS methods in the framework of finite element discretizations. For further discussions of VMS methods, we refer to reader to the survey on the VMS methods [22].

With the discrete inf–sup condition, GA-VMS formulation (2.6)–(2.7) can be computed equivalently solving: Find $(u_{h,1}^{n+1}, u_{h,2}^{n+1}, \mathbb{G}_1^{\mathbb{H},n+1}, \mathbb{G}_2^{\mathbb{H},n+1}) \in (V_1^h, V_2^h, L_1^H, L_2^H)$ such that

$$
\begin{aligned}
&(\frac{u_{h,1}^{n+1}-u_{h,1}^{n}}{\Delta t}, v_{h,1})_{\Omega_1} + (\nu_1+\nu_{T,1})(\nabla u_{h,1}^{n+1}, \nabla v_{h,1})_{\Omega_1} + c_1(u_{h,1}^{n+1}; u_{h,1}^{n+1}, v_{h,1}) \\
&\quad + \kappa \int_I |[\mathbf{u}_h^n]| u_{h,1}^{n+1} v_{h,1} ds - \kappa \int_I u_{h,2}^n |[\mathbf{u}_h^n]|^{1/2} |[\mathbf{u}_h^{n-1}]|^{1/2} v_{h,1} ds \\
&= (f_1^{n+1}, v_{h,1})_{\Omega_1} + \nu_{T,1}(\mathbb{G}_1^{\mathbb{H},n}, \nabla v_{h,1})_{\Omega_1}, \qquad (2.8) \\
&(\mathbb{G}_1^{\mathbb{H},n} - \nabla u_{h,1}^n, \mathbb{L}_1^H)_{\Omega_1} = 0, \qquad (2.9)
\end{aligned}
$$

and

$$
\begin{aligned}
&(\frac{u_{h,2}^{n+1}-u_{h,2}^{n}}{\Delta t}, v_{h,2})_{\Omega_2} + (\nu_2+\nu_{T,2})(\nabla u_{h,2}^{n+1}, \nabla v_{h,2}^h)_{\Omega_2} + c_2(u_{h,2}^{n+1}; u_{h,2}^{n+1}, v_{h,2}) \\
&\quad + \kappa \int_I |[\mathbf{u}_h^n]| u_{h,2}^{n+1} v_{h,2} ds - \kappa \int_I u_{h,1}^n |[\mathbf{u}_h^n]|^{1/2} |[\mathbf{u}_h^{n-1}]|^{1/2} v_{h,2} ds \\
&= (f_2^{n+1}, v_{h,2})_{\Omega_2} + \nu_{T,2}(\mathbb{G}_2^{\mathbb{H},n}, \nabla v_{h,2})_{\Omega_2}, \qquad (2.10) \\
&(\mathbb{G}_2^{\mathbb{H},n} - \nabla u_{h,2}^n, \mathbb{L}_2^H)_{\Omega_2} = 0, \qquad (2.11)
\end{aligned}
$$

for all $(v_{h,1}, v_{h,2}, \mathbb{L}_1^H, \mathbb{L}_2^H) \in (V_1^h, V_2^h, L_1^H, L_2^H)$.

Remark 2.2. Notice that the GA-VMS method (2.8)–(2.11) is derived, based on the variational formulation (2.1) — or, equivalently, one could derive (2.8)–(2.11) from (1.1)–(1.6), but the coefficients ν_i would need to be replaced with $\nu_i + \nu_{T,i}$ in (1.2). If, however, one tried to create a GA-VMS method from (1.1)–(1.6), all the interface integrals in (2.8)–(2.11) would be multiplied by $\frac{\nu_i+\nu_{T,i}}{\nu_i}$. Numerical tests show that this alternative approach fails to provide good quality approximations even for high ν_i values.

3. Mathematical preliminaries

In this section, some inequalities and definitions are introduced. The following lemmas are required for the analysis.

Lemma 3.1. *Let $\alpha, \beta, \theta \in H^1(\Omega_i)$ for $i = 1, 2$, then there exist constants $C(\Omega_i) > 0$ such that*

$$
\begin{aligned}
&c_i(\alpha; \beta, \theta) \le C(\Omega_i)\|\alpha\|_{\Omega_i}^{1/2} \|\nabla\alpha\|_{\Omega_i}^{1/2} \|\nabla\beta\|_{\Omega_i} \|\nabla\theta\|_{\Omega_i}, \\
&\int_I \alpha |[\beta]| \theta \le C(\Omega_i)\|\alpha\|_I \|[\beta]\|_I \|\theta\|_I, \\
&\quad \|\alpha\|_I \le C(\Omega_i)\left(\|\alpha\|_{\Omega_i}^{1/4} \|\nabla\alpha\|_{\Omega_i}^{3/4} + \|\alpha\|_{\Omega_i}^{1/6} \|\nabla\alpha\|_{\Omega_i}^{5/6} \right). \qquad (3.1)
\end{aligned}
$$

Proof. The first two bounds are standard — see, e.g., Lemma 2.1 on p. 1301 of [2]. The third bound can be found in [27], see Theorem II.4.1, p. 63. □

Lemma 3.2. *Let $\alpha_i \in X_i$, $\theta_j \in X_j$, $\boldsymbol{\beta} \in H^1(\Omega_i)$ and $\epsilon_i, \epsilon_j, \varepsilon_i, \varepsilon_j$ $(i, j = 1, 2)$ be positive constants, then one*

$$
\kappa \int_I |\alpha_i||[\boldsymbol{\beta}]||\theta_j| \le \frac{C\kappa^2}{4}\|\alpha_i\|_I^2 \|[\boldsymbol{\beta}]\|_I^2 + \frac{\epsilon_j}{\nu_j^5}\|\theta_j\|_{\Omega_j}^2 + \frac{\nu_j}{2\epsilon_j}\|\nabla\theta_j\|_{\Omega_j}^2, \qquad (3.2)
$$

$$
\begin{aligned}
\kappa \int_I |\alpha_i||[\boldsymbol{\beta}]||\theta_j| &\le C\kappa^6 \Big(\frac{\epsilon_i^5}{\nu_i^5} \|[\boldsymbol{\beta}]\|_I^6 \|\alpha_i\|_{\Omega_i}^2 + \frac{\varepsilon_j^5}{\nu_j^5} \|[\boldsymbol{\beta}]\|_I^6 \|\theta_j\|_{\Omega_j}^2 \Big) \\
&\quad + \frac{\nu_i}{4\epsilon_i}\|\nabla\alpha_i\|_{\Omega_i}^2 + \frac{\nu_j}{4\varepsilon_j}\|\nabla\theta_j\|_{\Omega_j}^2, \qquad (3.3)
\end{aligned}
$$

$$\kappa \int_I |\alpha_i||[\boldsymbol{\beta}]||\theta_j| \le C\kappa^6 \|\alpha_i\|_I^6 \Big(\frac{\epsilon_1^5}{\nu_1^5} \|\beta_1\|^2_{\Omega_1} + \frac{\epsilon_2^5}{\nu_2^5} \|\beta_2\|^2_{\Omega_2} + \frac{2\varepsilon_j^5}{\nu_j^5} \|\theta_j\|^2_{\Omega_j} \Big) + \frac{\nu_1}{4\epsilon_1} \|\nabla\beta_1\|^2_{\Omega_1} + \frac{\nu_2}{4\epsilon_2} \|\nabla\beta_2\|^2_{\Omega_2} + \frac{\nu_j}{2\beta_j} \|\nabla\theta_j\|^2_{\Omega_j}. \tag{3.4}$$

Proof. Use Lemma 3.1 and Young's inequality (see Lemma 2.2 on p. 1302 of [2]). □

Denoting the corresponding Galerkin approximations of (u_i, p_i) in (X_i^h, Q_i^h) by $(v_{h,i}, q_{h,i})$, one can assume that the following approximation assumptions (see [23]):

$$\inf_{v_{h,i} \in X_i^h} \Big(\|u_i - v_{h,i}\| + \|\nabla(u_i - v_{h,i})\| \Big) \le Ch^{k+1} \|u_i\|_{k+1}, \tag{3.5}$$

$$\inf_{q_{h,i} \in Q_i^h} \|p_i - q_{h,i}\| \le Ch^k \|p_i\|_k. \tag{3.6}$$

The L^2 projection is defined in the usual way.

Definition 3.1. The L^2 projection P^H of a given function $\mathbb{L}_i$ onto the finite element space L_i^H is the solution of the following : find $\hat{\mathbb{L}}_i = P^H \mathbb{L}_i \in L_i^H$ such that

$$(\mathbb{L}_i - P^H \mathbb{L}_i, S_H)_{\Omega_i} = 0, \tag{3.7}$$

for all $S_H \in L_i^H$.

Hence, we get

$$\|\mathbb{L}_i - P^H \mathbb{L}_i\|_{\Omega_i} \le CH^k \|\mathbb{L}_i\|_{k+1}, \tag{3.8}$$

for all $\mathbb{L} \in (L(\Omega_i))^{d\times d} \cap (H^{k+1}(\Omega_i))^{d\times d}$.

We also use Poincaré–Friedrichs inequality as: There exists a constant C_p such that

$$\|u_{h,i}\|_{\Omega_i} \le C_p \|\nabla u_{h,i}\|_{\Omega_i}, \quad \forall u_{h,i} \in X_i^h \tag{3.9}$$

holds. Along the paper, we use the following inequality whose proof can be found in [28].

Lemma 3.3 (*Discrete Gronwall Lemma*)**.** *Let $\gamma_i, \theta_i, \beta_i, \alpha_i$ (for $i \ge 0$), and Δt, C be a non-negative numbers such that*

$$\gamma_M + \Delta t \sum_{i=0}^{M} \theta_i \le \Delta t \sum_{i=0}^{M} \alpha_i \gamma_i + \Delta t \sum_{i=0}^{M} \beta_i + C, \ \forall M \ge 0.$$

Assume $\alpha_i \Delta t < 1$ for all i, then,

$$\gamma_M + \Delta t \sum_{i=0}^{M} \theta_i \le \exp\Big(\Delta t \sum_{i=0}^{M} \theta_i \frac{\alpha_i}{1 - \alpha_i \Delta t} \Big) \Big(\Delta t \sum_{i=0}^{M} \beta_i + C \Big), \ \forall M \ge 0.$$

4. Energy conservation and stability properties of GA-VMS method

This section considers the energy balance and the stability for the GA-VMS scheme. We first show that the scheme admits an energy balance which is analogous to balances for the continuous fluid–fluid interaction problem. Next, we prove its unconditional stability and long-time L^2 stability of velocity.

Lemma 4.1 (*Global Energy Conservation*)**.** *Let the starting values $u_{h,i}^0$ and $u_{h,i}^1$ be given. The scheme (2.8)–(2.11) admits the following energy conservation law:*

$$\|u_{h,1}^{M+1}\|^2_{\Omega_1} + \|u_{h,2}^{M+1}\|^2_{\Omega_2} + \Delta t \big(\nu_{T,1} \|\nabla u_{h,1}^{M+1}\|^2_{\Omega_1} + \nu_{T,2} \|\nabla u_{h,2}^{M+1}\|^2_{\Omega_2} \big)$$
$$+ \Delta t \sum_{n=1}^{M} (\|u_{h,1}^{n+1} - u_{h,1}^{n}\|^2_{\Omega_1} + \|u_{h,2}^{n+1} - u_{h,2}^{n}\|^2_{\Omega_2})$$

$$
\begin{aligned}
&+ \Delta t \sum_{n=1}^{M} \Big(2\nu_1 \|\nabla u_{h,1}^{n+1}\|_{\Omega_1}^2 + \nu_{T,1}\|\nabla u_{h,1}^{n+1} - \mathbb{G}_1^{\mathbb{H},n}\|_{\Omega_1}^2 + \nu_{T,1}\|\nabla u_{h,1}^{n} - \mathbb{G}_1^{\mathbb{H},n}\|_{\Omega_1}^2 \Big) \\
&+ \Delta t \sum_{n=1}^{M} \Big(2\nu_2 \|\nabla u_{h,2}^{n+1}\|_{\Omega_2}^2 + \nu_{T,2}\|\nabla u_{h,2}^{n+1} - \mathbb{G}_2^{\mathbb{H},n}\|_{\Omega_2}^2 + \nu_{T,2}\|\nabla u_{h,2}^{n} - \mathbb{G}_2^{\mathbb{H},n}\|_{\Omega_2}^2 \Big) \\
&+ \kappa \Delta t \int_I |[\mathbf{u}_h^M]|(|u_{h,1}^{M+1}|^2 + |u_{h,2}^{M+1}|^2) ds \\
&+ \kappa \Delta t \sum_{n=1}^{M} \int_I \Big| |[\mathbf{u}_h^n]|^{1/2} u_{h,1}^{n+1} - |[\mathbf{u}_h^{n-1}]|^{1/2} u_{h,2}^{n} \Big|^2 ds \\
&+ \kappa \Delta t \sum_{n=1}^{M} \int_I \Big| |[\mathbf{u}_h^n]|^{1/2} u_{h,2}^{n+1} - |[\mathbf{u}_h^{n-1}]|^{1/2} u_{h,1}^{n} \Big|^2 ds \\
= &\|u_{h,1}^1\|_{\Omega_1}^2 + \|u_{h,2}^1\|_{\Omega_2}^2 + \Delta t \big(\nu_{T,1}\|\nabla u_{h,1}^1\|_{\Omega_1}^2 + \nu_{T,2}\|\nabla u_{h,2}^1\|_{\Omega_2}^2\big) \\
&+ \kappa \Delta t \int_I |[u_h^0]|(|u_{h,1}^1|^2 + |u_{h,2}^1|^2) ds + 2\Delta t \sum_{n=1}^{M} (f_1^{n+1}, u_{h,1}^{n+1})_{\Omega_1} + 2\Delta t \sum_{n=1}^{M} (f_2^{n+1}, u_{h,2}^{n+1})_{\Omega_2}.
\end{aligned} \tag{4.1}
$$

Proof. Letting $v_{h,1} = u_{h,1}^{n+1}$ in (2.8) and $v_{h,2} = u_{h,2}^{n+1}$ in (2.10) and using the skew-symmetry property of nonlinear terms, we get

$$
\begin{aligned}
&(\frac{u_{h,1}^{n+1} - u_{h,1}^{n}}{\Delta t}, u_{h,1}^{n+1})_{\Omega_1} + (\nu_1 + \nu_{T,1})\|\nabla u_{h,1}^{n+1}\|_{\Omega_1}^2 \\
&\quad + \kappa \int_I |[\mathbf{u}_h^n]||u_{h,1}^{n+1}|^2 ds - \kappa \int_I u_{h,2}^{n} |[\mathbf{u}_h^n]|^{1/2} |[\mathbf{u}_h^{n-1}]|^{1/2} u_{h,1}^{n+1} ds \\
&= (f_1^{n+1}, u_{h,1}^{n+1})_{\Omega_1} + \nu_{T,1}(\mathbb{G}_1^{\mathbb{H},n}, \nabla u_{h,1}^{n+1})_{\Omega_1},
\end{aligned} \tag{4.2}
$$

and

$$
\begin{aligned}
&(\frac{u_{h,2}^{n+1} - u_{h,2}^{n}}{\Delta t}, u_{h,2}^{n+1})_{\Omega_2} + (\nu_2 + \nu_{T,2})\|\nabla u_{h,2}^{n+1}\|_{\Omega_2}^2 \\
&\quad + \kappa \int_I |[\mathbf{u}_h^n]||u_{h,2}^{n+1}|^2 ds - \kappa \int_I u_{h,1}^{n} |[\mathbf{u}_h^n]|^{1/2} |[\mathbf{u}_h^{n-1}]|^{1/2} u_{h,2}^{n+1} ds \\
&= (f_2^{n+1}, u_{h,2}^{n+1})_{\Omega_2} + \nu_{T,2}(\mathbb{G}_2^{\mathbb{H},n}, \nabla u_{h,2}^{n+1})_{\Omega_2}.
\end{aligned} \tag{4.3}
$$

Utilizing

$$
(a-b)\cdot a = \frac{1}{2}(|a|^2 + |a-b|^2 - |b|^2), \tag{4.4}
$$

we have

$$
\begin{aligned}
&\frac{1}{2\Delta t}(\|u_{h,1}^{n+1}\|_{\Omega_1}^2 + \|u_{h,1}^{n+1} - u_{h,1}^{n}\|_{\Omega_1}^2 - \|u_{h,1}^{n}\|_{\Omega_1}^2) \\
&\quad + (\nu_1 + \nu_{T,1})\|\nabla u_{h,1}^{n+1}\|_{\Omega_1}^2 - \nu_{T,1}(\mathbb{G}_1^{\mathbb{H},n}, \nabla u_{h,1}^{n+1})_{\Omega_1} \\
&\quad + \kappa \int_I |[\mathbf{u}_h^n]|\ |u_{h,1}^{n+1}|^2 ds - \kappa \int_I u_{h,2}^{n} |[\mathbf{u}_h^n]|^{1/2} [\mathbf{u}_h^{n-1}]^{1/2} u_{h,1}^{n+1} ds \\
&= (f_1^{n+1}, u_{h,1}^{n+1})_{\Omega_1},
\end{aligned} \tag{4.5}
$$

and

$$
\begin{aligned}
&\frac{1}{2\Delta t}(\|u_{h,2}^{n+1}\|_{\Omega_2}^2 + \|u_{h,2}^{n+1} - u_{h,2}^{n}\|_{\Omega_2}^2 - \|u_{h,2}^{n}\|_{\Omega_2}^2) \\
&\quad + (\nu_2 + \nu_{T,2})\|\nabla u_{h,2}^{n+1}\|_{\Omega_2}^2 - \nu_{T,2}(\mathbb{G}_2^{\mathbb{H},n}, \nabla u_{h,2}^{n+1})_{\Omega_2}
\end{aligned}
$$

$$
\begin{aligned}
&+\kappa\int_I |[\mathbf{u}_h^n]||u_{h,2}^{n+1}|^2 ds - \kappa\int_I u_{h,1}^n|[\mathbf{u}_h^n]|^{1/2}|[\mathbf{u}_h^{n-1}]|^{1/2}u_{h,2}^{n+1} ds\\
&= (f_2^{n+1}, u_{h,2}^{n+1})_{\Omega_2},
\end{aligned}
\tag{4.6}
$$

Adding (4.5) to (4.6) and multiplying by $2\Delta t$ yields

$$
\begin{aligned}
&\|u_{h,1}^{n+1}\|_{\Omega_1}^2 + \|u_{h,1}^{n+1} - u_{h,1}^n\|_{\Omega_1}^2 - \|u_{h,1}^n\|_{\Omega_1}^2 + \|u_{h,2}^{n+1}\|_{\Omega_2}^2 + \|u_{h,2}^{n+1} - u_{h,2}^n\|_{\Omega_2}^2 - \|u_{h,2}^n\|_{\Omega_2}^2\\
&\quad + 2\Delta t\Big((\nu_1+\nu_{T,1})\|\nabla u_{h,1}^{n+1}\|_{\Omega_1}^2 - \nu_{T,1}(\mathbb{G}_1^{\mathbb{H},n}, \nabla u_{h,1}^{n+1})_{\Omega_1} + (\nu_2+\nu_{T,2})\|\nabla u_{h,2}^{n+1}\|_{\Omega_2} - \nu_{T,2}(\mathbb{G}_2^{\mathbb{H},n}, \nabla u_{h,2}^{n+1})_{\Omega_2}\Big)\\
&\quad + 2\kappa\Delta t\int_I |[\mathbf{u}_h^n]||u_{h,1}^{n+1}|^2 ds + 2\kappa\Delta t\int_I |[\mathbf{u}_h^n]||u_{h,2}^{n+1}|^2 ds\\
&\quad - 2\kappa\Delta t\int_I u_{h,2}^n|[\mathbf{u}_h^n]|^{1/2}[\mathbf{u}_h^{n-1}]|^{1/2}u_{h,1}^{n+1} ds - 2\kappa\Delta t\int_I u_{h,1}^n|[\mathbf{u}_h^n]|^{1/2}|[\mathbf{u}_h^{n-1}]|^{1/2}u_{h,2}^{n+1} ds\\
&= 2\Delta t(f_1^{n+1}, u_{h,1}^{n+1})_{\Omega_1} + 2\Delta t(f_2^{n+1}, u_{h,2}^{n+1})_{\Omega_2}.
\end{aligned}
\tag{4.7}
$$

The interface terms on the left hand side of (4.7) can be expressed as (see [2])

$$
\begin{aligned}
&\kappa\int_I |[\mathbf{u}_h^n]|\ |u_{h,1}^{n+1}|^2 ds - \kappa\int_I u_{h,2}^n|[\mathbf{u}_h^n]|^{1/2}[\mathbf{u}_h^{n-1}]^{1/2}u_{h,1}^{n+1} ds\\
&\quad + \kappa\int_I |[\mathbf{u}_h^n]||u_{h,2}^{n+1}|^2 ds - \kappa\int_I u_{h,1}^n|[\mathbf{u}_h^n]|^{1/2}|[\mathbf{u}_h^{n-1}]|^{1/2}u_{h,2}^{n+1} ds\\
&= \frac{\kappa}{2}\int_I |[\mathbf{u}_h^n]|(|u_{h,1}^{n+1}|^2 + |u_{h,2}^{n+1}|^2) ds - \frac{\kappa}{2}\int_I |[\mathbf{u}_h^{n-1}]|(|u_{h,1}^n|^2 + |u_{h,2}^n|^2) ds\\
&\quad + \frac{\kappa}{2}\int_I \Big||[\mathbf{u}_h^n]|^{1/2}u_{h,1}^{n+1} - |[\mathbf{u}_h^{n-1}]|^{1/2}u_{h,2}^n\Big|^2 ds\\
&\quad + \frac{\kappa}{2}\int_I \Big||[\mathbf{u}_h^n]|^{1/2}u_{h,2}^{n+1} - |[\mathbf{u}_h^{n-1}]|^{1/2}u_{h,1}^n\Big|^2 ds.
\end{aligned}
\tag{4.8}
$$

Substituting (4.8) into (4.7) gives

$$
\begin{aligned}
&\|u_{h,1}^{n+1}\|_{\Omega_1}^2 + \|u_{h,1}^{n+1} - u_{h,1}^n\|_{\Omega_1}^2 - \|u_{h,1}^n\|_{\Omega_1}^2 + \|u_{h,2}^{n+1}\|_{\Omega_2}^2 + \|u_{h,2}^{n+1} - u_{h,2}^n\|_{\Omega_2}^2 - \|u_{h,2}^n\|_{\Omega_2}^2\\
&\quad + 2\Delta t\Big((\nu_1+\nu_{T,1})\|\nabla u_{h,1}^{n+1}\|_{\Omega_1}^2 - \nu_{T,1}(\mathbb{G}_1^{\mathbb{H},n}, \nabla u_{h,1}^{n+1})_{\Omega_1} + (\nu_2+\nu_{T,2})\|\nabla u_{h,2}^{n+1}\|_{\Omega_2} - \nu_{T,2}(\mathbb{G}_2^{\mathbb{H},n}, \nabla u_{h,2}^{n+1})_{\Omega_2}\Big)\\
&\quad + \kappa\Delta t\int_I |[\mathbf{u}_h^n]|(|u_{h,1}^{n+1}|^2 + |u_{h,2}^{n+1}|^2) ds - \kappa\Delta t\int_I |[\mathbf{u}_h^{n-1}]|(|u_{h,1}^n|^2 + |u_{h,2}^n|^2) ds\\
&\quad + \kappa\Delta t\int_I \Big||[\mathbf{u}_h^n]|^{1/2}u_{h,1}^{n+1} - |[\mathbf{u}_h^{n-1}]|^{1/2}u_{h,2}^n\Big|^2 ds + \kappa\Delta t\int_I \Big||[\mathbf{u}_h^n]|^{1/2}u_{h,2}^{n+1} - |[\mathbf{u}_h^{n-1}]|^{1/2}u_{h,1}^n\Big|^2 ds\\
&= 2\Delta t(f_1^{n+1}, u_{h,1}^{n+1})_{\Omega_1} + 2\Delta t(f_2^{n+1}, u_{h,2}^{n+1})_{\Omega_2},
\end{aligned}
\tag{4.9}
$$

Also considering the fact that $(\nabla u_{h,i}^n - \mathbb{G}_i^{\mathbb{H},n}, \mathbb{G}_i^{\mathbb{H},n})_{\Omega_i} = 0$, one can easily show

$$
\|\nabla u_{h,i}^n - \mathbb{G}_i^{\mathbb{H},n}\|_{\Omega_i}^2 = \|\nabla u_{h,i}^n\|_{\Omega_i}^2 - \|\mathbb{G}_i^{\mathbb{H},n}\|_{\Omega_i}^2.
$$

The last equality and some algebraic manipulations give

$$
\begin{aligned}
&(\nu_i+\nu_{T,i})\|\nabla u_{h,i}^{n+1}\|_{\Omega_i}^2 - \nu_{T,i}(\mathbb{G}_i^{\mathbb{H},n}, \nabla u_{h,i}^{n+1})_{\Omega_i}\\
&= \nu_i\|\nabla u_{h,i}^{n+1}\|_{\Omega_i}^2 + \frac{\nu_{T,i}}{2}\big(\|\nabla u_{h,i}^{n+1} - \mathbb{G}_i^{\mathbb{H},n}\|_{\Omega_i}^2 + 2(\mathbb{G}_i^{\mathbb{H},n}, \nabla u_{h,i}^{n+1})_{\Omega_i} - \|\mathbb{G}_i^{\mathbb{H},n}\|_{\Omega_i}^2\big)\\
&\quad - \nu_{T,i}(\mathbb{G}_i^{\mathbb{H},n}, \nabla u_{h,i}^{n+1})_{\Omega_i} + \frac{\nu_{T,i}}{2}\big(\|\nabla u_{h,i}^{n+1}\|_{\Omega_i}^2 - \|\nabla u_{h,i}^n\|_{\Omega_i}^2\big) + \frac{\nu_{T,i}}{2}\|\nabla u_{h,i}^n\|_{\Omega_i}^2\\
&= \nu_i\|\nabla u_{h,i}^{n+1}\|_{\Omega_i}^2 + \frac{\nu_{T,i}}{2}\|\nabla u_{h,i}^{n+1} - \mathbb{G}_i^{\mathbb{H},n}\|_{\Omega_i}^2 + \frac{\nu_{T,i}}{2}\|\nabla u_{h,i}^n - \mathbb{G}_i^{\mathbb{H},n}\|_{\Omega_i}^2\\
&\quad + \frac{\nu_{T,i}}{2}\big(\|\nabla u_{h,i}^{n+1}\|_{\Omega_i}^2 - \|\nabla u_{h,i}^n\|_{\Omega_i}^2\big).
\end{aligned}
$$

Substituting the last equation in (4.9),

$$\begin{aligned}
&\|u_{h,1}^{n+1}\|_{\Omega_1}^2 + \|u_{h,1}^{n+1} - u_{h,1}^n\|_{\Omega_1}^2 - \|u_{h,1}^n\|_{\Omega_1}^2 + \|u_{h,2}^{n+1}\|_{\Omega_2}^2 + \|u_{h,2}^{n+1} - u_{h,2}^n\|_{\Omega_2}^2 - \|u_{h,2}^n\|_{\Omega_2}^2 \\
&\quad + \Delta t\Big(2\nu_1\|\nabla u_{h,1}^{n+1}\|_{\Omega_1}^2 + \nu_{T,1}\|\nabla u_{h,1}^{n+1} - \mathbb{G}_1^{\mathbb{H},n}\|_{\Omega_1}^2 \\
&\quad + \nu_{T,1}\|\nabla u_{h,1}^n - \mathbb{G}_1^{\mathbb{H},n}\|_{\Omega_1}^2 + \nu_{T,1}\big(\|\nabla u_{h,1}^{n+1}\|_{\Omega_1}^2 - \|\nabla u_{h,1}^n\|_{\Omega_1}^2\big)\Big) \\
&\quad + \Delta t\Big(2\nu_2\|\nabla u_{h,2}^{n+1}\|_{\Omega_2}^2 + \nu_{T,2}\|\nabla u_{h,2}^{n+1} - \mathbb{G}_2^{\mathbb{H},n}\|_{\Omega_2}^2 \\
&\quad + \nu_{T,2}\|\nabla u_{h,2}^n - \mathbb{G}_2^{\mathbb{H},n}\|_{\Omega_2}^2 + \nu_{T,2}\big(\|\nabla u_{h,2}^{n+1}\|_{\Omega_2}^2 - \|\nabla u_{h,2}^n\|_{\Omega_2}^2\big)\Big) \\
&\quad + \kappa\Delta t\int_I |[\mathbf{u}_h^n]|(|u_{h,1}^{n+1}|^2 + |u_{h,2}^{n+1}|^2)ds - \kappa\Delta t\int_I |[\mathbf{u}_h^{n-1}]|(|u_{h,1}^n|^2 + |u_{h,2}^n|^2)ds \\
&\quad + \kappa\Delta t\int_I \Big||[\mathbf{u}_h^n]|^{1/2}u_{h,1}^{n+1} - |[\mathbf{u}_h^{n-1}]|^{1/2}u_{h,2}^n\Big|^2 ds + \kappa\Delta t\int_I \Big||[\mathbf{u}_h^n]|^{1/2}u_{h,2}^{n+1} - |[\mathbf{u}_h^{n-1}]|^{1/2}u_{h,1}^n\Big|^2 ds \\
&= 2\Delta t(f_1^{n+1}, u_{h,1}^{n+1})_{\Omega_1} + 2\Delta t(f_2^{n+1}, u_{h,2}^{n+1})_{\Omega_2}, \qquad (4.10)
\end{aligned}$$

Summing over the time levels completes the proof. □

We now provide the stability of (2.8)–(2.11).

Lemma 4.2. *Let $f_i \in L^2(0,T;H^{-1}(\Omega_i))$ for $i = 1,2$. The scheme (2.8)–(2.11) is unconditionally stable and provides the following bound at time step $t = M+1$*

$$\begin{aligned}
&\|u_{h,1}^{M+1}\|_{\Omega_1}^2 + \|u_{h,2}^{M+1}\|_{\Omega_2}^2 + \Delta t(\nu_{T,1}\|\nabla u_{h,1}^{M+1}\|_{\Omega_1}^2 + \nu_{T,2}\|\nabla u_{h,2}^{M+1}\|_{\Omega_2}^2) \\
&\quad + \Delta t\sum_{n=1}^M\Big(\nu_1\|\nabla u_{h,1}^{n+1}\|_{\Omega_1}^2 + \nu_{T,1}\|\nabla u_{h,1}^{n+1} - \mathbb{G}_1^{\mathbb{H},n}\|_{\Omega_1}^2 + \nu_{T,1}\|\nabla u_{h,1}^n - \mathbb{G}_1^{\mathbb{H},n}\|_{\Omega_1}^2\Big) \\
&\quad + \Delta t\sum_{n=1}^M\Big(\nu_2\|\nabla u_{h,2}^{n+1}\|_{\Omega_2}^2 + \nu_{T,2}\|\nabla u_{h,2}^{n+1} - \mathbb{G}_2^{\mathbb{H},n}\|_{\Omega_2}^2 + \nu_{T,2}\|\nabla u_{h,2}^n - \mathbb{G}_2^{\mathbb{H},n}\|_{\Omega_2}^2\Big) \\
&\quad + \kappa\Delta t\int_I |[\mathbf{u}_h^M]|(|u_{h,1}^{M+1}|^2 + |u_{h,2}^{M+1}|^2)ds \\
&\quad + \kappa\Delta t\sum_{n=1}^M\int_I \Big||[\mathbf{u}_h^n]|^{1/2}u_{h,1}^{n+1} - |[\mathbf{u}_h^{n-1}]|^{1/2}u_{h,2}^n\Big|^2 ds \\
&\quad + \kappa\Delta t\sum_{n=1}^M\int_I \Big||[\mathbf{u}_h^n]|^{1/2}u_{h,2}^{n+1} - |[\mathbf{u}_h^{n-1}]|^{1/2}u_{h,1}^n\Big|^2 ds \\
&\le \|u_{h,1}^1\|_{\Omega_1}^2 + \|u_{h,2}^1\|_{\Omega_2}^2 + \kappa\Delta t\int_I |[u_h^0]|(|u_{h,1}^1|^2 + |u_{h,2}^1|^2)ds + \Delta t(\nu_{T,1}\|\nabla u_{h,1}^1\|_{\Omega_1}^2 + \nu_{T,2}\|\nabla u_{h,2}^1\|_{\Omega_2}^2) \\
&\quad + \Delta t\sum_{n=1}^M(\nu_1^{-1}\|f_1^{n+1}\|_{-1,\Omega_1}^2 + \nu_2^{-1}\|f_2^{n+1}\|_{-1,\Omega_2}^2) \qquad (4.11)
\end{aligned}$$

Proof. Performing Cauchy–Schwarz and Young's inequalities for the last two terms on the right side of energy conservation equation (4.1), we have

$$2\Delta t\sum_{n=1}^M(f_1^{n+1}, u_{h,1}^{n+1})_{\Omega_1} \le \nu_1^{-1}\Delta t\sum_{n=1}^M\|f_1^{n+1}\|_{-1,\Omega_1}^2 + \nu_1\Delta t\sum_{n=1}^M\|\nabla u_{h,1}^{n+1}\|_{\Omega_1}^2, \qquad (4.12)$$

$$2\Delta t\sum_{n=1}^M(f_2^{n+1}, u_{h,2}^{n+1})_{\Omega_2} \le \nu_2^{-1}\Delta t\sum_{n=1}^M\|f_2^{n+1}\|_{-1,\Omega_2}^2 + \nu_2\Delta t\sum_{n=1}^M\|\nabla u_{h,2}^{n+1}\|_{\Omega_2}^2. \qquad (4.13)$$

Substituting (4.12)–(4.13) in (4.1) and dropping non-negative terms produces the required result. □

We next prove that (2.8)–(2.11) is unconditionally long-time stable. To perform the long-time stability, in view of Lemma 4.2, the right-hand side of (4.11) is denoted by S_M,

$$S_M := \|u_{h,1}^1\|_{\Omega_1}^2 + \|u_{h,2}^1\|_{\Omega_2}^2 + \kappa\Delta t\int_I |[u_h^0]|(|u_{h,1}^1|^2 + |u_{h,2}^1|^2)ds + \Delta t(\nu_{T,1}\|\nabla u_{h,1}^1\|_{\Omega_1}^2 + \nu_{T,2}\|\nabla u_{h,2}^1\|_{\Omega_2}^2)$$
$$+\Delta t\sum_{n=1}^{M}(\nu_1^{-1}\|f_1^{n+1}\|_{-1,\Omega_1}^2 + \nu_2^{-1}\|f_2^{n+1}\|_{-1,\Omega_2}^2). \tag{4.14}$$

Lemma 4.3. *Let $f_i \in L^\infty(\mathbb{R}^+, V_i^{h*})$ for $i = 1, 2$ be given, then solutions of the scheme (2.8)–(2.11) are long-time stable in the following sense: for any time step $\Delta t > 0$ and for any $n > 0$*

$$\|u_{h,1}^{n+1}\|_{\Omega_1}^2 + \nu_{T,1}\Delta t\|\nabla u_{h,1}^{n+1}\|_{\Omega_1}^2 + \kappa\Delta t\int_I |[\mathbf{u}_h^n]|(|u_{h,1}^{n+1}|^2)ds$$
$$+ \|u_{h,2}^{n+1}\|_{\Omega_2}^2 + \nu_{T,2}\Delta t\|\nabla u_{h,2}^{n+1}\|_{\Omega_2}^2 + \kappa\Delta t\int_I |[\mathbf{u}_h^n]|(|u_{h,2}^{n+1}|^2)ds$$
$$\leq (1+\alpha)^{-n}\Big(\|u_{h,1}^1\|_{\Omega_1}^2 + \nu_{T,1}\Delta t\|\nabla u_{h,1}^1\|_{\Omega_1}^2 + \kappa\Delta t\int_I |[\mathbf{u}_h^0]|(|u_{h,1}^1|^2)ds$$
$$+ \|u_{h,2}^1\|_{\Omega_2}^2 + \nu_{T,2}\Delta t\|\nabla u_{h,2}^1\|_{\Omega_2}^2 + \kappa\Delta t\int_I |[\mathbf{u}_h^0]|(|u_{h,2}^1|^2)ds\Big)$$
$$+\alpha^{-1}\Delta t(\nu_1^{-1}\|f_1\|_{L^\infty(\mathbb{R}^+,V_1^{h*})}^2 + \nu_2^{-1}\|f_2\|_{L^\infty(\mathbb{R}^+,V_2^{h*})}^2), \tag{4.15}$$

where $\alpha := \min\Big\{\frac{\nu_i\Delta t}{3C_p^2}, \frac{\nu_i}{3\nu_{T,i}}, \frac{\nu_i}{3}(\frac{C\kappa^2 S_M}{4} + \frac{2C_p^2}{\nu_i^5} + \frac{\nu_i}{4})^{-1}\Big\}$, *for* $i = 1, 2$.

Proof. Letting $\mathbb{L}_i^H = \mathbb{G}_i^{\mathbb{H},n}$ in (2.9) and (2.11) and utilizing Cauchy–Schwarz inequality gives

$$\|\mathbb{G}_i^{\mathbb{H},n}\|_{\Omega_i} \leq \|\nabla u_{h,i}^n\|_{\Omega_i}. \tag{4.16}$$

Adding (4.5) to (4.6), applying Cauchy–Schwarz and Young's inequalities, using (4.8), (4.16), multiplying by $2\Delta t$ and dropping the non-negative terms, we have

$$\|u_{h,1}^{n+1}\|_{\Omega_1}^2 + \nu_{T,1}\Delta t\|\nabla u_{h,1}^{n+1}\|_{\Omega_1}^2 + \kappa\Delta t\int_I |[\mathbf{u}_h^n]|(|u_{h,1}^{n+1}|^2)ds$$
$$+ \|u_{h,2}^{n+1}\|_{\Omega_2}^2 + \nu_{T,2}\Delta t\|\nabla u_{h,2}^{n+1}\|_{\Omega_2}^2 + \kappa\Delta t\int_I |[\mathbf{u}_h^n]|(|u_{h,2}^{n+1}|^2)ds$$
$$+ \nu_1\Delta t\|\nabla u_{h,1}^{n+1}\|_{\Omega_1}^2 + \nu_2\Delta t\|\nabla u_{h,2}^{n+1}\|_{\Omega_2}^2$$
$$\leq \|u_{h,1}^n\|_{\Omega_1}^2 + \nu_{T,1}\Delta t\|\nabla u_{h,1}^n\|_{\Omega_1}^2 + \kappa\Delta t\int_I |[\mathbf{u}_h^{n-1}]|(|u_{h,1}^n|^2)ds$$
$$+ \|u_{h,2}^n\|_{\Omega_2}^2 + \nu_{T,2}\Delta t\|\nabla u_{h,2}^n\|_{\Omega_2}^2 + \kappa\Delta t\int_I |[\mathbf{u}_h^{n-1}]|(|u_{h,2}^n|^2)ds$$
$$+ \Delta t\nu_1^{-1}\|f_1^{n+1}\|_{V_1^{h*}}^2 + \Delta t\nu_2^{-1}\|f_2^{n+1}\|_{V_1^{h*}}^2. \tag{4.17}$$

Using Lemma 3.2 with $\varepsilon = 2$, Poincaré inequality and Lemma 4.2 produce

$$\kappa\int_I |[\mathbf{u}_h^n]||u_{h,i}^{n+1}|^2 \leq \frac{C\kappa^2}{4}|[\mathbf{u}_h^n]|_I^2|u_{h,i}^{n+1}|_I^2 + (\frac{2C_p^2}{\nu_i^5} + \frac{\nu_i}{4})\|\nabla u_{h,i}^{n+1}\|^2$$
$$\leq \frac{C\kappa^2}{4}|[\mathbf{u}_h^n]|_I^2\|u_{h,i}^{n+1}\|_{\Omega_i}^{1/3}\|\nabla u_{h,i}^{n+1}\|_{\Omega_i}^{5/3} + (\frac{2C_p^2}{\nu_i^5} + \frac{\nu_i}{4})\|\nabla u_{h,i}^{n+1}\|_{\Omega_i}^2$$
$$\leq (\frac{C\kappa^2 S_M}{4} + \frac{2C_p^2}{\nu_i^5} + \frac{\nu_i}{4})\|\nabla u_{h,i}^{n+1}\|_{\Omega_i}^2, \quad \text{for } i = 1, 2, \tag{4.18}$$

where S_M has been defined in (4.14). Thus, the last two terms on the left hand side of (4.17) can be written as

$$\nu_1 \Delta t \|\nabla u_{h,1}^{n+1}\|_{\Omega_1}^2 + \nu_2 \Delta t \|\nabla u_{h,2}^{n+1}\|_{\Omega_2}^2$$
$$\geq \alpha \Big(\|u_{h,1}^{n+1}\|_{\Omega_1}^2 + \nu_{T,1} \Delta t \|\nabla u_{h,1}^{n+1}\|_{\Omega_1}^2 + \kappa \Delta t \int_I |[\mathbf{u}_h^n]| (|u_{h,1}^{n+1}|^2) ds$$
$$+ \|u_{h,2}^{n+1}\|_{\Omega_2}^2 + \nu_{T,2} \Delta t \|\nabla u_{h,2}^{n+1}\|_{\Omega_2}^2 + \kappa \Delta t \int_I |[\mathbf{u}_h^n]| (|u_{h,2}^{n+1}|^2) ds \Big), \tag{4.19}$$

where $\alpha := \min\Big\{ \frac{\nu_i \Delta t}{3C_p^2}, \frac{\nu_i}{3\nu_{T,i}}, \frac{\nu_i}{3}(\frac{C\kappa^2 S_M}{4} + \frac{2C_p^2}{\nu_i^5} + \frac{\nu_i}{4})^{-1} \Big\}$, for $i = 1, 2$. Inserting (4.19) in (4.17) and multiplying by $(1+\alpha)^{-1}$, we obtain

$$\|u_{h,1}^{n+1}\|_{\Omega_1}^2 + \nu_{T,1} \Delta t \|\nabla u_{h,1}^{n+1}\|_{\Omega_1}^2 + \kappa \Delta t \int_I |[\mathbf{u}_h^n]| (|u_{h,1}^{n+1}|^2) ds$$
$$+ \|u_{h,2}^{n+1}\|_{\Omega_2}^2 + \nu_{T,2} \Delta t \|\nabla u_{h,2}^{n+1}\|_{\Omega_2}^2 + \kappa \Delta t \int_I |[\mathbf{u}_h^n]| (|u_{h,2}^{n+1}|^2) ds$$
$$\leq (1+\alpha)^{-1} \Big(\|u_{h,1}^n\|_{\Omega_1}^2 + \nu_{T,1} \Delta t \|\nabla u_{h,1}^n\|_{\Omega_1}^2 + \kappa \Delta t \int_I |[\mathbf{u}_h^{n-1}]| (|u_{h,1}^n|^2) ds$$
$$+ \|u_{h,2}^n\|_{\Omega_2}^2 + \nu_{T,2} \Delta t \|\nabla u_{h,2}^n\|_{\Omega_2}^2 + \kappa \Delta t \int_I |[\mathbf{u}_h^{n-1}]| (|u_{h,2}^n|^2) ds \Big)$$
$$+ \Delta t \nu_1^{-1} (1+\alpha)^{-1} \|f_1^{n+1}\|_{V_1^{h*}}^2 + \Delta t \nu_2^{-1} (1+\alpha)^{-1} \|f_2^{n+1}\|_{V_1^{h*}}^2. \tag{4.20}$$

Utilizing induction produces the stated result (4.15). □

Remark 4.1. Lemma 4.3 proves that the long-time velocity solutions are bounded by the problem data and this bound is weakly dependent on the initial conditions when n is sufficiently large. In the limit, as $n \to \infty$, this upper bound on the problem data becomes independent of the initial conditions.

5. Convergence analysis

This section presents convergence analysis of (2.8)–(2.10). It is assumed that all functions are sufficiently regular, i.e. the solution of (1.1)–(1.6) satisfies

$$u \in L^\infty(0, T; H^{k+1}(\Omega) \cap H^3(\Omega)), \quad \partial_t u \in L^\infty(0, T; H^{k+1}(\Omega)^d), \quad \partial_{tt} u \in L^\infty(0, T; H^1(\Omega)^d). \tag{5.1}$$

We need to define the following discrete norms to use in the convergence analysis.

$$|||u|||_{\infty,p} = \max_{0 \leq j \leq N} \|u(t^j)\|_p, \;\; |||u|||_{s,p} = \Big(\Delta t \sum_{j=1}^{M} \|u(t^j)\|_p^s \Big)^{\frac{1}{s}}. \tag{5.2}$$

Following the notation of [2], let $D^{n+1} = \tilde{\nu}^5 \Big(1 + \kappa^6 E^{n+1} + |||\nabla u|||_{\infty,\Omega}^4 + (\nu_{T,1}^2 + \nu_{T,2}^2) h^{-2} \Big)$, where $\tilde{\nu} = \max\{(\nu_1 + \nu_{T,1})^{-1}, (\nu_2 + \nu_{T,2})^{-1}\}$ and $E^{n+1} = \max_{j=0,1,\ldots,n+1}\{\max\{\|u(t^j)\|_I^6, \|u_h^j\|_I^6\}\}$.

Theorem 5.1. *Let the time step be chosen so that $\Delta t \leq 1/D^{n+1}$. Then the following bound on the error holds under the regularity assumptions (5.1):*

$$\|\mathbf{u}(t^{M+1}) - \mathbf{u}^{M+1}\|^2 + \frac{3}{4}(\nu_1 + \nu_{T,1}) \Delta t \sum_{n=1}^{M} \|\nabla (u_1(t^{n+1}) - u_{h,1}^{n+1})\|^2$$
$$+ 2\kappa \Delta t \sum_{n=1}^{M} \int_I |[\mathbf{u}^n]| |\mathbf{u}(t^{n+1}) - \mathbf{u}^{n+1}|^2 ds + \frac{3}{4}(\nu_2 + \nu_{T,2}) \Delta t \sum_{n=1}^{M} \|\nabla (u_2(t^{n+1}) - u_{h,2}^{n+1})\|^2$$
$$\leq \|\mathbf{u}(t^1) - \mathbf{u}_h^1\|^2 + \frac{(\nu_1 + \nu_{T,1})\Delta t}{8} (2\|\nabla (u_1(t^1) - u_{h,1}^1)\|_{\Omega_1}^2 + \|\nabla (u_1(t^0) - u_{h,1}^0)\|_{\Omega_1}^2)$$

$$+\frac{(\nu_2+\nu_{T,2})\Delta t}{8}(2\|\nabla(u_2(t^1)-u_{h,2}^1)\|_{\Omega_2}^2+\|\nabla(u_2(t^0)-u_{h,2}^0)\|_{\Omega_2}^2)$$
$$+C(\Delta t^2+h^{2k}+(\nu_{T,2}^2(\nu_2+\nu_{T,2})^{-1}+\nu_{T,1}^2(\nu_1+\nu_{T,1})^{-1})H^{2k}), \tag{5.3}$$

where C is a generic constant depending only on $f_i, \nu_i+\nu_{T,i}, \Omega$.

Proof. The finite element error analysis starts by deriving error equations for GA-VMS finite element method (2.8)–(2.10) by subtracting the scheme from weak formulation of (1.1)–(1.6) . To do this, first note that the true solution of (1.1)–(1.6) at time t^{n+1} satisfies

$$\begin{aligned}
&(\frac{u_1(t^{n+1})-u_1(t^n)}{\Delta t},v_{h,1})_{\Omega_1}+(\nu_1+\nu_{T,1})(\nabla u_1(t^{n+1}),\nabla v_{h,1})_{\Omega_1}-(p_1(t^{n+1}),\nabla\cdot v_{h,1})_{\Omega_1}\\
&+\kappa\int_I(u_1(t^{n+1})-u_2(t^{n+1}))|[\mathbf{u}(t^{n+1})]|v_{h,1}ds+c_1(u_1(t^{n+1});u_1(t^{n+1}),v_{h,1})\\
&=(\frac{u_1(t^{n+1})-u_1(t^n)}{\Delta t}-\partial_t u_1(t^{n+1}),v_{h,1})_{\Omega_1}+\nu_{T,1}(\nabla u_1(t^{n+1}),\nabla v_{h,1})_{\Omega_1}\\
&+(f_1^{n+1},v_{h,1})_{\Omega_1}
\end{aligned}\tag{5.4}$$

and

$$\begin{aligned}
&(\frac{u_2(t^{n+1})-u_2(t^n)}{\Delta t},v_{h,2})_{\Omega_2}+(\nu_2+\nu_{T,2})(\nabla u_2(t^{n+1}),\nabla v_{h,2})_{\Omega_2}-(p_2(t^{n+1}),\nabla\cdot v_{h,2})_{\Omega_2}\\
&+\kappa\int_I(u_2(t^{n+1})-u_1(t^{n+1}))|[\mathbf{u}(t^{n+1})]|v_{h,2}ds+c_2(u_2(t^{n+1});u_2(t^{n+1}),v_{h,2})\\
&=(\frac{u_2(t^{n+1})-u_2(t^n)}{\Delta t}-\partial_t u_2(t^{n+1}),v_{h,2})_{\Omega_2}+\nu_{T,2}(\nabla u_2(t^{n+1}),\nabla v_{h,2})_{\Omega_2}\\
&+(f_2^{n+1},v_{h,2})_{\Omega_2},
\end{aligned}\tag{5.5}$$

for all $(v_{h,1},v_{h,2})\in(V_1^h,V_2^h)$. For arbitrary $\tilde{u}_1^{n+1}\in V_1^h$ and $\tilde{u}_2^{n+1}\in V_2^h$, the error is decomposed into

$$\begin{aligned}
e_1^{n+1}&=u_1(t^{n+1})-u_{h,1}^{n+1}=(u_1(t^{n+1})-\tilde{u_1}^{n+1})-(u_{h,1}^{n+1}-\tilde{u_1}^{n+1})=:\eta_1^{n+1}-\phi_{h,1}^{n+1},\\
e_2^{n+1}&=u_2(t^{n+1})-u_{h,2}^{n+1}=(u_2(t^{n+1})-\tilde{u_2}^{n+1})-(u_{h,2}^{n+1}-\tilde{u_2}^{n+1})=:\eta_2^{n+1}-\phi_{h,2}^{n+1}.
\end{aligned}\tag{5.6}$$

The interpolation error can be estimated with (3.5). Thus, subtracting (2.8)–(2.11) from (5.4)–(5.5) gives

$$\begin{aligned}
&(\frac{\phi_{h,1}^{n+1}-\phi_{h,1}^n}{\Delta t},v_{h,1})_{\Omega_1}+(\nu_1+\nu_{T,1})(\nabla\phi_{h,1}^{n+1},\nabla v_{h,1})_{\Omega_1}+\kappa\int_I|[\mathbf{u}_h^n]|u_{h,1}^{n+1}v_{h,1}ds\\
&-\kappa\int_I|[\mathbf{u}(t^{n+1})]|u_1(t^{n+1})v_{h,1}ds+\kappa\int_I u_2(t^{n+1})|[\mathbf{u}(t^{n+1})]|v_{h,1}ds\\
&-\kappa\int_I u_{h,2}^n|[\mathbf{u}_h^n]|^{1/2}|[\mathbf{u}_h^{n-1}]|^{1/2}v_{h,1}ds\\
&=(\frac{\eta_1^{n+1}-\eta_1^n}{\Delta t},v_{h,1})_{\Omega_1}+(\nu_1+\nu_{T,1})(\nabla\eta_1^{n+1},\nabla v_{h,1})_{\Omega_1}-(p_1(t^{n+1})-q_{h,1}^{n+1},\nabla\cdot v_{h,1})_{\Omega_1}\\
&+(\partial_t u_1(t^{n+1})-\frac{u_1(t^{n+1})-u_1(t^n)}{\Delta t},v_{h,1})_{\Omega_1}+\nu_{T,1}(\mathbb{G}_1^{\mathbb{H},n}-\nabla u_1(t^{n+1}),\nabla v_{h,1})_{\Omega_1}\\
&+c_1(u_1(t^{n+1});u_1(t^{n+1}),v_{h,1})-c_1(u_{h,1}^{n+1};u_{h,1}^{n+1},v_{h,1}),
\end{aligned}\tag{5.7}$$

and

$$\begin{aligned}
&(\frac{\phi_{h,2}^{n+1}-\phi_{h,2}^n}{\Delta t},v_{h,2})_{\Omega_2}+(\nu_2+\nu_{T,2})(\nabla\phi_{h,2}^{n+1},\nabla v_{h,2})_{\Omega_2}+\kappa\int_I|[\mathbf{u}_h^n]|u_{h,2}^{n+1}v_{h,2}ds\\
&-\kappa\int_I|[\mathbf{u}(t^{n+1})]|u_2(t^{n+1})v_{h,2}ds+\kappa\int_I u_1(t^{n+1})|[\mathbf{u}(t^{n+1})]|v_{h,2}ds\\
&-\kappa\int_I u_{h,1}^n|[\mathbf{u}_h^n]|^{1/2}|[\mathbf{u}_h^{n-1}]|^{1/2}v_{h,2}ds
\end{aligned}$$

$$
\begin{aligned}
&= (\frac{\eta_2^{n+1}-\eta_2^n}{\Delta t}, v_{h,2})_{\Omega_2} + (\nu_2+\nu_{T,2})(\nabla\eta_2^{n+1}, \nabla v_{h,2})_{\Omega_2} - (p_2(t^{n+1}) - q_{h,2}^{n+1}, \nabla\cdot v_{h,2})_{\Omega_2} \\
&+ (\partial_t u_2(t^{n+1}) - \frac{u_2(t^{n+1})-u_2(t^n)}{\Delta t}, v_{h,2})_{\Omega_2} + \nu_{T,2}(\mathbb{G}_2^{\mathbb{H},n} - \nabla u_2(t^{n+1}), \nabla v_{h,2})_{\Omega_2} \\
&+ c_2(u_2(t^{n+1}); u_2(t^{n+1}), v_{h,2}) - c_2(u_{h,2}^{n+1}; u_{h,2}^{n+1}, v_{h,2}).
\end{aligned} \tag{5.8}
$$

Then choosing $v_{h,1} = \phi_{h,1}^{n+1}$ in (5.7) and using the polarization identity (4.4) provides

$$
\begin{aligned}
&\frac{1}{2\Delta t}\Big(\|\phi_{h,1}^{n+1}\|_{\Omega_1}^2 - \|\phi_{h,1}^n\|_{\Omega_1}^2 + \|\phi_{h,1}^{n+1}-\phi_{h,1}^n\|_{\Omega_1}^2\Big) + (\nu_1+\nu_{T,1})\|\nabla\phi_{h,1}^{n+1}\|_{\Omega_1} \\
&+ \kappa\int_I |[\mathbf{u}_h^n]| u_{h,1}^{n+1}\phi_{h,1}^{n+1} ds - \kappa\int_I |[\mathbf{u}(t^{n+1})]| u_1(t^{n+1})\phi_{h,1}^{n+1} ds \\
&+ \kappa\int_I u_2(t^{n+1})|[\mathbf{u}(t^{n+1})]|\phi_{h,1}^{n+1} ds - \kappa\int_I u_{h,2}^n |[\mathbf{u}_h^n]|^{1/2} |[\mathbf{u}_h^{n-1}]|^{1/2}\phi_{h,1}^{n+1} ds \\
&\le \left|(\frac{\eta_1^{n+1}-\eta_1^n}{\Delta t}, \phi_{h,1}^{n+1})_{\Omega_1}\right| + (\nu_1+\nu_{T,1})\left|(\nabla\eta_1^{n+1}, \nabla\phi_{h,1}^{n+1})_{\Omega_1}\right| + \left|(p_1(t^{n+1}) - q_{h,1}^{n+1}, \nabla\cdot\phi_{h,1}^{n+1})_{\Omega_1}\right| \\
&+ \left|(\partial_t u_1(t^{n+1}) - \frac{u_1(t^{n+1})-u_1(t^n)}{\Delta t}, \phi_{h,1}^{n+1})_{\Omega_1}\right| + \nu_{T,1}\left|(\mathbb{G}_1^{\mathbb{H},n} - \nabla u_1(t^{n+1}), \nabla\phi_{h,1}^{n+1})_{\Omega_1}\right| \\
&+ c_1(u_1(t^{n+1}); u_1(t^{n+1}), \phi_{h,1}^{n+1}) - c_1(u_{h,1}^{n+1}; u_{h,1}^{n+1}, \phi_{h,1}^{n+1}).
\end{aligned} \tag{5.9}
$$

Applying Cauchy–Schwarz, Young's, and Poincaré inequalities along with Taylor theorem, we get

$$
\begin{aligned}
\left|(\frac{\eta_1^{n+1}-\eta_1^n}{\Delta t}, \phi_{h,1}^{n+1})_{\Omega_1}\right| &\le C(\nu_1+\nu_{T,1})^{-1}\Delta t^{-1}\int_{t^n}^{t^{n+1}} \|\partial_t\eta_1^{n+1}\|_{\Omega_1}^2 \\
&+ \frac{(\nu_1+\nu_{T,1})}{36}\|\nabla\phi_{h,1}^{n+1}\|_{\Omega_1}^2, \qquad (5.10)\\
(\nu_1+\nu_{T,1})\left|(\nabla\eta_1^{n+1}, \nabla\phi_{h,1}^{n+1})_{\Omega_1}\right| &\le C(\nu_1+\nu_{T,1})\|\nabla\eta_1^{n+1}\|_{\Omega_1}^2 \\
&+ \frac{(\nu_1+\nu_{T,1})}{36}\|\nabla\phi_{h,1}^{n+1}\|_{\Omega_1}^2, \qquad (5.11)\\
\left|(p_1(t^{n+1}) - q_{h,1}^{n+1}, \nabla\cdot\phi_{h,1}^{n+1})_{\Omega_1}\right| &\le C(\nu_1+\nu_{T,1})^{-1}\|p_1(t^{n+1}) - q_{h,1}^{n+1}\|_{\Omega_1}^2 \\
&+ \frac{(\nu_1+\nu_{T,1})}{36}\|\nabla\phi_{h,1}^{n+1}\|_{\Omega_1}^2, \qquad (5.12)\\
\left|(\partial_t u_1(t^{n+1}) - \frac{u_1(t^{n+1})-u_1(t^n)}{\Delta t}, \phi_{h,1}^{n+1})_{\Omega_1}\right| &\le C(\nu_1+\nu_{T,1})^{-1}\|\partial_t u_1(t^{n+1}) - \frac{u_1(t^{n+1})-u_1(t^n)}{\Delta t}\|_{\Omega_1}^2 \\
&+ \frac{(\nu_1+\nu_{T,1})}{36}\|\nabla\phi_{h,1}^{n+1}\|_{\Omega_1}^2. \qquad (5.13)
\end{aligned}
$$

Eqs. (2.9) and (2.11) state that $\mathbb{G}_i^{\mathbb{H},n} = P^H\nabla u_{h,i}^n$ where P^H is the $L^2(\Omega_i)$-orthogonal projection defined by (3.7). Hence, utilizing Cauchy–Schwarz and Young's inequality to the fifth term on the right hand side of (5.9) yields

$$
\begin{aligned}
&\nu_{T,1}\left|(\mathbb{G}_1^{\mathbb{H},n} - \nabla u_1(t^{n+1}), \nabla\phi_{h,1}^{n+1})_{\Omega_1}\right| \\
&\le \nu_{T,1}(P^H\nabla(u_{h,1}^n - u_1(t^n)), \nabla\phi_{h,1}^{n+1})_{\Omega_1} - \nu_{T,1}((I-P^H)\nabla u_1(t^n), \nabla\phi_{h,1}^{n+1})_{\Omega_1} \\
&- \nu_{T,1}(\nabla(u_1(t^{n+1}) - u_1(t^n)), \nabla\phi_{h,1}^{n+1})_{\Omega_1} \\
&\le C{\nu_{T,1}}^2(\nu_1+\nu_{T,1})^{-1}\Big(\|P^H\nabla\eta_1^n\|_{\Omega_1}^2 + \|P^H\nabla\phi_{h,1}^n\|_{\Omega_1}^2 \\
&+ \|(I-P^H)\nabla u_1(t^n)\|_{\Omega_1}^2 + \|\nabla(u_1(t^{n+1}) - u_1(t^n))\|_{\Omega_1}^2\Big) \\
&+ \frac{\nu_1+\nu_{T,1}}{36}\|\nabla\phi_{h,1}^{n+1}\|_{\Omega_1}^2.
\end{aligned} \tag{5.14}
$$

Taylor remainder formula is used along with (3.7), (3.8) and inverse inequality to get

$$\begin{aligned}
&\nu_{T,1}\left|(\mathbb{G}_1^{\mathbb{H},n}-\nabla u_1(t^{n+1}),\nabla\phi_{h,1}^{n+1})_{\Omega_1}\right| \\
&\le C{\nu_{T,1}}^2(\nu_1+\nu_{T,1})^{-1}\Big(\|\nabla\eta_1^n\|^2+h^{-2}\|\phi_{h,1}^n\|^2+H^{2k}\|u_1(t^n)\|_{k+1}^2 \\
&\quad+\Delta t^2\|\partial_t u_1\|^2_{L^\infty(t^n,t^{n+1};H^1(\Omega))}\Big)+\frac{\nu_1+\nu_{T,1}}{36}\|\nabla\phi_{h,1}^{n+1}\|^2_{\Omega_1}. \qquad (5.15)
\end{aligned}$$

The nonlinear terms can be rearranged by adding and subtracting terms and using $c_1(u_{h,1}^{n+1};\phi_{h,1}^{n+1},\phi_{h,1}^{n+1})=0$ as follows.

$$\begin{aligned}
&c_1(u_1(t^{n+1});u_1(t^{n+1}),\phi_{h,1}^{n+1})-c_1(u_{h,1}^{n+1};u_{h,1}^{n+1},\phi_{h,1}^{n+1}) \\
&=c_1(\eta_1^{n+1};u_1(t^{n+1}),\phi_{h,1}^{n+1})-c_1(\phi_{h,1}^{n+1};u_1(t^{n+1}),\phi_{h,1}^{n+1}) \\
&\quad+c_1(u_{h,1}^{n+1};\eta_1^{n+1},\phi_{h,1}^{n+1}). \qquad (5.16)
\end{aligned}$$

Bounds for the terms on the right hand side of (5.16) are given as

$$\begin{aligned}
c_1(\eta_1^{n+1};u_1(t^{n+1}),\phi_{h,1}^{n+1}) &\le C(\nu_1+\nu_{T,1})^{-1}\|\nabla\eta_1^{n+1}\|^2_{\Omega_1}\|\nabla u_1(t^{n+1})\|^2_{\Omega_1} \\
&\quad+\frac{(\nu_1+\nu_{T,1})}{36}\|\nabla\phi_{h,1}^{n+1}\|^2_{\Omega_1}, \\
c_1(\phi_{h,1}^{n+1};u_1(t^{n+1}),\phi_{h,1}^{n+1}) &\le C\|\phi_{h,1}^{n+1}\|^{1/2}_{\Omega_1}\|\nabla\phi_{h,1}^{n+1}\|^{1/2}_{\Omega_1}\|\nabla u_1(t^{n+1})\|_{\Omega_1}\|\nabla\phi_{h,1}^{n+1}\|_{\Omega_1} \\
&\le C(\nu_1+\nu_{T,1})^{-3}\|\phi_{h,1}^{n+1}\|^2_{\Omega_1}\|\nabla u_1(t^{n+1})\|^4_{\Omega_1} \\
&\quad+\frac{(\nu_1+\nu_{T,1})}{36}\|\nabla\phi_{h,1}^{n+1}\|^2_{\Omega_1}, \\
c_1(u_{h,1}^{n+1};\eta_1^{n+1},\phi_{h,1}^{n+1}) &\le C(\nu_1+\nu_{T,1})^{-1}\|\nabla\eta_1^{n+1}\|^2_{\Omega_1}\|\nabla u_{h,1}^{n+1}\|^2_{\Omega_1} \\
&\quad+\frac{(\nu_1+\nu_{T,1})}{36}\|\nabla\phi_{h,1}^{n+1}\|^2_{\Omega_1}. \qquad (5.17)
\end{aligned}$$

The interface integrals can be expressed as

$$\begin{aligned}
&\kappa\int_I|[\mathbf{u}_h^n]|u_{h,1}^{n+1}\phi_{h,1}^{n+1}ds-\kappa\int_I|[\mathbf{u}(t^{n+1})]|u_1(t^{n+1})\phi_{h,1}^{n+1}ds \\
&=-\kappa\int_I|[\mathbf{u}_h^n]||\phi_{h,1}^{n+1}|^2ds+\kappa\int_I|[\mathbf{u}_h^n]|\eta_1^{n+1}\phi_{h,1}^{n+1}ds \\
&\quad+\kappa\int_I(|[\mathbf{u}_h^n]|-|[\tilde{\mathbf{u}}^n]|)u_1(t^{n+1})\phi_{h,1}^{n+1}ds \\
&\quad+\kappa\int_I(|[\tilde{\mathbf{u}}^n]|-|[\mathbf{u}(t^n)]|)u_1(t^{n+1})\phi_{h,1}^{n+1}ds \\
&\quad+\kappa\int_I(|[\mathbf{u}(t^n)]|-|[\mathbf{u}(t^{n+1})]|)u_1(t^{n+1})\phi_{h,1}^{n+1}ds, \qquad (5.18)
\end{aligned}$$

and

$$\begin{aligned}
&\kappa\int_I u_2(t^{n+1})|[\mathbf{u}(t^{n+1})]|\phi_{h,1}^{n+1}ds-\kappa\int_I u_{h,2}^n|[\mathbf{u}^n]|^{1/2}|[\mathbf{u}^{n-1}]|^{1/2}\phi_{h,1}^{n+1}ds \\
&=\kappa\int_I(u_2(t^{n+1})-u_2(t^n))|[\mathbf{u}(t^{n+1})]|\phi_{h,1}^{n+1}ds+\kappa\int_I(\phi_{h,2}^n-\eta_2^n)|[\mathbf{u}(t^{n+1})]|\phi_{h,1}^{n+1}ds \\
&\quad+\kappa\int_I u_{h,2}^n\Big(|[\mathbf{u}(t^{n+1})]|-\frac{1}{2}(|[\mathbf{u}(t^n)]|+|[\mathbf{u}(t^{n-1})]|)\Big)\phi_{h,1}^{n+1}ds \\
&\quad+\kappa\int_I u_{h,2}^n\Big(\frac{1}{2}(|[\mathbf{u}(t^n)]|+|[\mathbf{u}(t^{n-1})]|-\frac{1}{2}(|[\tilde{\mathbf{u}}^n]|+|[\tilde{\mathbf{u}}^{n-1}]|))\Big)\phi_{h,1}^{n+1}ds \\
&\quad+\kappa\int_I u_{h,2}^n\Big(\frac{1}{2}(|[\tilde{\mathbf{u}}^n]|+|[\tilde{\mathbf{u}}^{n-1}]|)-\frac{1}{2}(|[\mathbf{u}_h^n]|+|[\mathbf{u}_h^{n-1}]|)\Big)\phi_{h,1}^{n+1}ds \\
&\quad+\kappa\int_I u_{h,2}^n\Big(\frac{1}{2}(|[\mathbf{u}_h^n]|+|[\mathbf{u}_h^{n-1}]|)-|[\mathbf{u}_h^n]|^{1/2}|[\mathbf{u}_h^{n-1}]|^{1/2}\Big)\phi_{h,1}^{n+1}ds. \qquad (5.19)
\end{aligned}$$

With the use of Lemma 3.2 and the following inequalities

$$\Big| |[\mathbf{u}(t^n)]| - |[\tilde{\mathbf{u}}^n]| \Big| \leq |[\boldsymbol{\eta}^n]|,$$
$$\Big| |[\mathbf{u}_h^n]| - |[\tilde{\mathbf{u}}^n]| \Big| \leq |[\boldsymbol{\phi}_h^n]|, \tag{5.20}$$

we bound the terms on the right hand side of (5.18) as

$$\kappa \int_I |\eta_1^{n+1}||[\mathbf{u}_h^n]||\phi_{h,1}^{n+1}|ds \leq \frac{C\kappa^2}{4}\|\eta_1^{n+1}\|_I^2\|[\mathbf{u}_h^n]\|_I^2 + C(\nu_1+\nu_{T,1})^{-5}\|\phi_{h,1}^{n+1}\|_{\Omega_1}^2 + \frac{(\nu_1+\nu_{T,1})}{36}\|\nabla\phi_{h,1}^{n+1}\|_{\Omega_1}^2, \tag{5.21}$$

$$\begin{aligned}\kappa \int_I |u_1(t^{n+1})|(|[\mathbf{u}_h^n]| - |[\tilde{\mathbf{u}}^n]|)|\phi_{h,1}^{n+1}|ds &\leq C\kappa^6\|u_1(t^{n+1})\|_I^6\Big((\nu_1+\nu_{T,1})^{-5}\|\phi_{h,1}^n\|_{\Omega_1}^2 + (\nu_2+\nu_{T,2})^{-5}\|\phi_{h,2}^n\|_{\Omega_2}^2 \\ &\quad + (\nu_1+\nu_{T,1})^{-5}\|\phi_{h,1}^{n+1}\|_{\Omega_1}^2\Big) + \frac{(\nu_1+\nu_{T,1})}{32}\|\nabla\phi_{h,1}^n\|_{\Omega_1}^2 \\ &\quad + \frac{(\nu_2+\nu_{T,2})}{48}\|\nabla\phi_{h,2}^n\|_{\Omega_2}^2 + \frac{(\nu_1+\nu_{T,1})}{36}\|\nabla\phi_{h,1}^{n+1}\|_{\Omega_1}^2,\end{aligned} \tag{5.22}$$

$$\begin{aligned}\kappa \int_I |u_1(t^{n+1})|(|[\tilde{\mathbf{u}}^n]| - |[\mathbf{u}(t^n)]|)|\phi_{h,1}^{n+1}|ds &\leq \frac{C\kappa^2}{4}\|u_1(t^{n+1})\|_I^2\|[\boldsymbol{\eta}^n]\|_I^2 + C(\nu_1+\nu_{T,1})^{-5}\|\phi_{h,1}^{n+1}\|_{\Omega_1}^2 \\ &\quad + \frac{(\nu_1+\nu_{T,1})}{36}\|\nabla\phi_{h,1}^{n+1}\|_{\Omega_1}^2,\end{aligned} \tag{5.23}$$

$$\begin{aligned}\kappa \int_I |u_1(t^{n+1})||[\mathbf{u}(t^n) - \mathbf{u}(t^{n+1})]||\phi_{h,1}^{n+1}|ds &\leq \frac{C\kappa^2}{4}\|u_1(t^{n+1})\|_I^2\|[\mathbf{u}(t^n) - \mathbf{u}(t^{n+1})]\|_I^2 + C(\nu_1+\nu_{T,1})^{-5}\|\phi_{h,1}^{n+1}\|_{\Omega_1}^2 \\ &\quad + \frac{(\nu_1+\nu_{T,1})}{36}\|\nabla\phi_{h,1}^{n+1}\|_{\Omega_1}^2.\end{aligned} \tag{5.24}$$

Similarly, the first six terms on the right hand side of (5.19) become

$$\begin{aligned}\kappa \int_I |u_2(t^{n+1}) - u_2(t^n)||[\mathbf{u}(t^{n+1})]||\phi_{h,1}^{n+1}|ds &\leq \frac{C\kappa^2}{4}\|u_2(t^{n+1}) - u_2(t^n)\|_I^2\|[\mathbf{u}(t^{n+1})]\|_I^2 + C(\nu_1+\nu_{T,1})^{-5}\|\phi_{h,1}^{n+1}\|_{\Omega_1}^2 \\ &\quad + \frac{(\nu_1+\nu_{T,1})}{36}\|\nabla\phi_{h,1}^{n+1}\|_{\Omega_1}^2,\end{aligned} \tag{5.25}$$

$$\begin{aligned}\kappa \int_I |\phi_{h,2}^n||[\mathbf{u}(t^{n+1})]||\phi_{h,1}^{n+1}|ds &\leq C\kappa^6\|[\mathbf{u}(t^{n+1})]\|_I^6\Big((\nu_2+\nu_{T,2})^{-5}\|\phi_{h,2}^n\|_{\Omega_2}^2 + (\nu_1+\nu_{T,1})^{-5}\|\phi_{h,1}^{n+1}\|_{\Omega_1}^2\Big) \\ &\quad + \frac{(\nu_2+\nu_{T,2})}{48}\|\nabla\phi_{h,2}^n\|_{\Omega_2}^2 + \frac{(\nu_1+\nu_{T,1})}{36}\|\nabla\phi_{h,1}^{n+1}\|_{\Omega_1}^2,\end{aligned} \tag{5.26}$$

$$\begin{aligned}\kappa \int_I |\eta_2^n||[\mathbf{u}(t^{n+1})]||\phi_{h,1}^{n+1}|ds &\leq \frac{C\kappa^2}{4}\|\eta_2^n\|_I^2\|[\mathbf{u}(t^{n+1})]\|_I^2 + C(\nu_1+\nu_{T,1})^{-5}\|\phi_{h,1}^{n+1}\|_{\Omega_1}^2 \\ &\quad + \frac{(\nu_1+\nu_{T,1})}{36}\|\nabla\phi_{h,1}^{n+1}\|_{\Omega_1}^2,\end{aligned} \tag{5.27}$$

$$\kappa\int_I |u^n_{h,2}|\Big(|[\mathbf{u}(t^{n+1})]| - \frac{1}{2}(|[\mathbf{u}(t^n)]| + |[\mathbf{u}(t^{n-1})]|)\Big)|\phi^{n+1}_{h,1}|ds$$
$$\le \frac{\kappa}{2}\int_I |u^n_{h,2}|\Big(|[\mathbf{u}(t^n)-\mathbf{u}(t^{n+1})]| + |[\mathbf{u}(t^{n-1})-\mathbf{u}(t^{n+1})]|\Big)|\phi^{n+1}_{h,1}|ds$$
$$\le \frac{C\kappa^2}{8}\|u^n_{h,2}\|^2_I\Big(|[\mathbf{u}(t^n)-\mathbf{u}(t^{n+1})]|^2_I + |[\mathbf{u}(t^{n-1})-\mathbf{u}(t^{n+1})]|^2_I\Big)$$
$$+ C(\nu_1+\nu_{T,1})^{-5}\|\phi^{n+1}_{h,1}\|^2_{\Omega_1} + \frac{(\nu_1+\nu_{T,1})}{36}\|\nabla\phi^{n+1}_{h,1}\|^2_{\Omega_1}, \tag{5.28}$$

$$\frac{\kappa}{2}\int_I |u^n_{h,2}|\Big(|[\mathbf{u}(t^n)]| + |[\mathbf{u}(t^{n-1})]| - |[\tilde{\mathbf{u}}^n]| - |[\tilde{\mathbf{u}}^{n-1}]|\Big)|\phi^{n+1}_{h,1}|ds$$
$$\le \frac{C\kappa^2}{8}\|u^n_{h,2}\|^2_I(\|[\boldsymbol{\eta}^n]\|^2_I + \|[\boldsymbol{\eta}^{n-1}]\|^2_I) + C(\nu_1+\nu_{T,1})^{-5}\|\phi^{n+1}_{h,1}\|^2_{\Omega_1}$$
$$+ \frac{(\nu_1+\nu_{T,1})}{36}\|\nabla\phi^{n+1}_{h,1}\|^2_{\Omega_1}, \tag{5.29}$$

$$\frac{\kappa}{2}\int_I |u^n_{h,2}|\Big(|[\tilde{\mathbf{u}}^n]| + |[\tilde{\mathbf{u}}^{n-1}]| - |[\mathbf{u}^n_h]| - |[\mathbf{u}^{n-1}_h]|\Big)|\phi^{n+1}_{h,1}|ds$$
$$\le C\kappa^6\|u^n_{h,2}\|^6_I\Big((\nu_1+\nu_{T,1})^{-5}\|\boldsymbol{\phi}^n_{h,1}\|^2_{\Omega_1} + (\nu_2+\nu_{T,2})^{-5}\|\boldsymbol{\phi}^n_{h,2}\|^2_{\Omega_2} + (\nu_1+\nu_{T,1})^{-5}\|\boldsymbol{\phi}^{n-1}_{h,1}\|^2_{\Omega_1}$$
$$+ (\nu_2+\nu_{T,2})^{-5}\|\boldsymbol{\phi}^{n-1}_{h,2}\|^2_{\Omega_2} + (\nu_1+\nu_{T,1})^{-5}\|\phi^{n+1}_{h,1}\|^2_{\Omega_1}\Big) + \Big(\frac{(\nu_1+\nu_{T,1})}{32}\|\nabla\boldsymbol{\phi}^n_{h,1}\|^2_{\Omega_1}$$
$$+ \frac{(\nu_2+\nu_{T,2})}{48}\|\nabla\boldsymbol{\phi}^n_{h,2}\|^2_{\Omega_2} + \frac{(\nu_1+\nu_{T,1})}{16}\|\nabla\boldsymbol{\phi}^{n-1}_{h,1}\|^2_{\Omega_1} + \frac{(\nu_2+\nu_{T,2})}{16}\|\nabla\boldsymbol{\phi}^{n-1}_{h,2}\|^2_{\Omega_2}$$
$$+ \frac{(\nu_1+\nu_{T,1})}{36}\|\nabla\phi^{n+1}_{h,1}\|^2_{\Omega_1}\Big). \tag{5.30}$$

The last term of (5.19) can be written as

$$\kappa\int_I |u^n_{h,2}|\Big(\frac{1}{2}(|[\mathbf{u}^n_h]| + |[\mathbf{u}^{n-1}_h]|) - |[\mathbf{u}^n_h]|^{1/2}|[\mathbf{u}^{n-1}_h]|^{1/2}\Big)|\phi^{n+1}_{h,1}|ds$$
$$\le \frac{\kappa}{2}\int_I |u^n_{h,2}|\Big(|[\boldsymbol{\phi}^n_h]| + |[\boldsymbol{\phi}^{n-1}_h]| + |[\boldsymbol{\eta}^n]| + |[\boldsymbol{\eta}^{n-1}]| + |[\mathbf{u}(t^n)-\mathbf{u}(t^{n-1})]|\Big)|\phi^{n+1}_{h,1}|ds, \tag{5.31}$$

which can be bounded in a similar way to (5.29) and (5.30). Inserting all bounds in (5.9) and multiplying by $2\Delta t$ gives

$$\|\phi^{n+1}_{h,1}\|^2_{\Omega_1} - \|\phi^n_{h,1}\|^2_{\Omega_1} + \|\phi^{n+1}_{h,1} - \phi^n_{h,1}\|^2_{\Omega_1} + (\nu_1+\nu_{T,1})\Delta t\|\nabla\phi^{n+1}_{h,1}\|_{\Omega_1}$$
$$+ 2\kappa\Delta t\int_I |[\mathbf{u}^n_h]||\phi^{n+1}_{h,1}|^2 ds - \frac{\nu_1+\nu_{T,1}}{8}\Delta t(\|\nabla\boldsymbol{\phi}^n_{h,1}\|^2_{\Omega_1} + \|\nabla\boldsymbol{\phi}^{n-1}_{h,1}\|^2_{\Omega_1})$$
$$- \frac{\nu_2+\nu_{T,1}}{8}\Delta t(\|\nabla\boldsymbol{\phi}^n_{h,2}\|^2_{\Omega_2} + \|\nabla\boldsymbol{\phi}^{n-1}_{h,2}\|^2_{\Omega_2})$$
$$\le C\Delta t\Big(\Delta t^{-1}\int_{t^n}^{t^{n+1}}\|\partial_t\eta^{n+1}_1\|^2_{\Omega_1} + \Big(1 + \|\nabla u_1(t^{n+1})\|^2_{\Omega_1} + \|\nabla u^{n+1}_{h,1}\|^2_{\Omega_1}\Big)\|\nabla\eta^{n+1}_1\|^2$$
$$+ \|p_1(t^{n+1}) - q^{n+1}_{h,1}\|^2_{\Omega_1} + \|\partial_t u_1(t^{n+1}) - \frac{u_1(t^{n+1}) - u_1(t^n)}{\Delta t}\|^2_{\Omega_1} + \|\nabla\eta^n_1\|^2_{\Omega_1}$$
$$+ {\nu_{T,1}}^2(\nu_1+\nu_{T,1})^{-1}H^{2k}\|u_1(t^n)\|^2_{k+1} + \Delta t^2\|\partial_t u_1\|^2_{L^\infty(t^n,t^{n+1};H^1(\Omega))}$$
$$+ \|\eta^{n+1}_1\|^2_I\|[\mathbf{u}^n_h]\|^2_I + \|u_1(t^{n+1})\|^2_I\|[\boldsymbol{\eta}^n]\|^2_I$$
$$+ \|u_1(t^{n+1})\|^2_I\|[\mathbf{u}(t^n) - \mathbf{u}(t^{n+1})]\|^2_I + \|u_2(t^{n+1}) - u_2(t^n)\|^2_I\|[\mathbf{u}(t^{n+1})]\|^2_I$$
$$+ \|\eta^n_2\|^2_I\|[\mathbf{u}(t^{n+1})]\|^2_I + \|u^n_{h,2}\|^2_I(\|[\boldsymbol{\eta}^n]\|^2_I + \|[\boldsymbol{\eta}^{n-1}]\|^2_I)$$
$$+ \|u^n_{h,2}\|^2_I\Big(|[\mathbf{u}(t^n) - \mathbf{u}(t^{n+1})]|^2_I + |[\mathbf{u}(t^{n-1}) - \mathbf{u}(t^{n+1})]|^2_I + |[\mathbf{u}(t^n) - \mathbf{u}(t^{n-1})]|^2_I\Big)\Big)$$

$$
\begin{aligned}
&+C(\nu_1+\nu_{T,1})^{-5}\Big(1+\|\nabla u_1(t^{n+1})\|^4_{\Omega_1}+\kappa^6(\|u_1(t^{n+1})\|_I^6+\|[\mathbf{u}(t^{n+1})]\|_I^6\\
&+\|u^n_{h,2}\|_I^6)\Big)\|\phi^{n+1}_{h,1}\|^2_{\Omega_1}+C\kappa^6\Big((\nu_1+\nu_{T,1})^{-5}(\|u_1(t^{n+1})\|_I^6+\|u^n_{h,2}\|_I^6)+\nu^2_{T,1}h^{-2}\Big)\|\phi^n_{h,1}\|^2_{\Omega_1}\\
&+C\kappa^6(\nu_1+\nu_{T,1})^{-5}\Big(\|u_1(t^{n+1})\|_I^6+\|u^n_{h,2}\|_I^6+\|[\mathbf{u}(t^{n+1})]\|_I^6\Big)\|\phi^n_{h,2}\|^2_{\Omega_2}\\
&+C\kappa^6(\nu_1+\nu_{T,1})^{-5}\|u^n_{h,2}\|_I^6\Big(\|\boldsymbol{\phi}^{n-1}_{h,1}\|^2_{\Omega_1}+\|\boldsymbol{\phi}^{n-1}_{h,2}\|^2_{\Omega_2}\Big). \qquad (5.32)
\end{aligned}
$$

Under the interpolation estimates (3.5), (3.6) and Lemma 3.1, the terms on the right hand side of (5.32) can be expressed as

$$
\begin{aligned}
\int_{t^n}^{t^{n+1}}\|\partial_t\eta_1^{n+1}\|^2_{\Omega_1}&\le Ch^{2k+2}\|\partial_t u_1\|^2_{L^2(t^n,t^{n+1};H^{k+1}(\Omega))}, &(5.33)\\
\|\eta_i^{n+1}\|_I^2\le C\|\nabla\eta_i^{n+1}\|^2_{\Omega_i}&\le Ch^{2k}\|u_i\|^2_{k+1,\Omega_i}, &(5.34)\\
\|\eta_i^{n+1}\|^2_{\Omega_i}&\le Ch^{2k+2}\|u_i\|^2_{k+1,\Omega_i}, &(5.35)\\
\|p_1(t^{n+1})-q^{n+1}_{h,1}\|^2_{\Omega_1}&\le Ch^{2k}\|p_1\|^2_{k,\Omega_1}, &(5.36)\\
\Delta t\|\partial_t u_1-\frac{u_1(t^{n+1})-u_1(t^n)}{\Delta t}\|^2_{\Omega_1}&\le C\Delta t^2\|\partial_{tt}u_1\|^2_{L^\infty(t^n,t^{n+1};L^2(\Omega))}, &(5.37)
\end{aligned}
$$

for $i=1,2$. Substituting (5.33)–(5.37) into (5.32) and summing over the time steps yield

$$
\begin{aligned}
&\|\phi^{M+1}_{h,1}\|^2_{\Omega_1}-\|\phi^1_{h,1}\|^2_{\Omega_1}+\sum_{n=1}^M\|\phi^{n+1}_{h,1}-\phi^n_{h,1}\|^2_{\Omega_1}+(\nu_1+\nu_{T,1})\Delta t\sum_{n=1}^M\|\nabla\phi^{n+1}_{h,1}\|_{\Omega_1}\\
&+2\kappa\Delta t\sum_{n=1}^M\int_I|[\mathbf{u}^n_h]||\phi^{n+1}_{h,1}|^2ds-\frac{\nu_1+\nu_{T,1}}{8}\Delta t\sum_{n=1}^M(\|\nabla\boldsymbol{\phi}^n_{h,1}\|^2_{\Omega_1}+\|\nabla\boldsymbol{\phi}^{n-1}_{h,1}\|^2_{\Omega_1})\\
&-\frac{\nu_2+\nu_{T,2}}{8}\Delta t\sum_{n=1}^M(\|\nabla\boldsymbol{\phi}^n_{h,2}\|^2_{\Omega_2}+\|\nabla\boldsymbol{\phi}^{n-1}_{h,2}\|^2_{\Omega_2})\\
&\le C\Big(h^{2k+2}\|\partial_t u_1\|^2_{L^2(0,T;H^{k+1}(\Omega_1))}+h^{2k}(1+|||\nabla u_1|||^2_{\infty,\Omega_1}+S_M)|||u_1|||^2_{2,k+1}+h^{2k}|||p_1|||^2_{2,k}\\
&+\Delta t^2(\|\partial_{tt}u_1\|^2_{L^\infty(0,T;L^2(\Omega_1))}+\|\partial_t u_1\|^2_{L^\infty(0,T;H^1(\Omega))})+{\nu_{T,1}}^2(\nu_1+\nu_{T,1})^{-1}H^{2k}|||u_1|||^2_{2,k+1}\\
&+h^{2k}(|||u_1|||^2_{\infty,I}+S_M)|||[\boldsymbol{u}]|||^2_{2,k+1}+h^{2k}(S_M|||u_1|||^2_{2,k+1}+\|[\mathbf{u}]\|^2_{\infty,I}|||u_2|||^2_{2,k+1})\\
&+C(\nu_1+\nu_{T,1})^{-5}\Big(1+|||\nabla u_1|||^4_{\infty,\Omega_1}+\kappa^6(|||u_1|||^6_{\infty,I}+\|[\mathbf{u}]\|^6_{\infty,I}+S_M)\Big)\Delta t\sum_{n=1}^M\|\phi^{n+1}_{h,1}\|^2_{\Omega_1}\\
&+C\Big(\kappa^6(\nu_1+\nu_{T,1})^{-5}(|||u_1|||^6_{\infty,I}+S_M)+\nu^2_{T,1}h^{-2}\Big)\Delta t\sum_{n=1}^M\|\phi^n_{h,1}\|^2_{\Omega_1}\\
&+C\kappa^6(\nu_1+\nu_{T,1})^{-5}\Big(|||u_1|||^6_{\infty,I}+S_M+\|[\mathbf{u}]\|^6_{\infty,I}\Big)\Delta t\sum_{n=1}^M\|\phi^n_{h,2}\|^2_{\Omega_2}\\
&+C\kappa^6(\nu_1+\nu_{T,1})^{-5}S_M\Delta t\sum_{n=1}^M\Big(\|\boldsymbol{\phi}^{n-1}_{h,1}\|^2_{\Omega_1}+\|\boldsymbol{\phi}^{n-1}_{h,2}\|^2_{\Omega_2}\Big)\Big) \qquad (5.38)
\end{aligned}
$$

where S_M represents to right hand side of (4.11). Simplifying (5.38), we have

$$
\begin{aligned}
&\|\phi^{M+1}_{h,1}\|^2_{\Omega_1}-\|\phi^1_{h,1}\|^2_{\Omega_1}+\sum_{n=1}^M\|\phi^{n+1}_{h,1}-\phi^n_{h,1}\|^2_{\Omega_1}+(\nu_1+\nu_{T,1})\Delta t\sum_{n=1}^M\|\nabla\phi^{n+1}_{h,1}\|_{\Omega_1}\\
&+2\kappa\Delta t\sum_{n=1}^M\int_I|[\mathbf{u}^n_h]||\phi^{n+1}_{h,1}|^2ds-\frac{\nu_1+\nu_{T,1}}{8}\Delta t\sum_{n=1}^M(\|\nabla\boldsymbol{\phi}^n_{h,1}\|^2_{\Omega_1}+\|\nabla\boldsymbol{\phi}^{n-1}_{h,1}\|^2_{\Omega_1})
\end{aligned}
$$

$$
\begin{aligned}
&- \frac{\nu_2 + \nu_{T,2}}{8} \Delta t \sum_{n=1}^{M} (\|\nabla \boldsymbol{\phi}_{h,2}^{n}\|_{\Omega_2}^2 + \|\nabla \boldsymbol{\phi}_{h,2}^{n-1}\|_{\Omega_2}^2) \\
&\leq C(\Delta t^2 + h^{2k} + \nu_{T,1}{}^2(\nu_1 + \nu_{T,1})^{-1} H^{2k}) \\
&\quad + C(\nu_1 + \nu_{T,1})^{-5}\Big(1 + \|\!|\nabla u_1|\!\|_{\infty,\Omega_1}^4 + \kappa^6(\|\!|u_1|\!\|_{\infty,I}^6 + \|[\mathbf{u}]\|_{\infty,I}^6 + S_M)\Big) \Delta t \sum_{n=1}^{M} \|\phi_{h,1}^{n+1}\|_{\Omega_1}^2 \\
&\quad + C\Big(\kappa^6(\nu_1 + \nu_{T,1})^{-5}(\|\!|u_1|\!\|_{\infty,I}^6 + S_M) + \nu_{T,1}^2 h^{-2}\Big) \Delta t \sum_{n=1}^{M} \|\phi_{h,1}^{n}\|_{\Omega_1}^2 \\
&\quad + C\kappa^6(\nu_1 + \nu_{T,1})^{-5}\Big(\|\!|u_1|\!\|_{\infty,I}^6 + S_M + \|[\mathbf{u}]\|_{\infty,I}^6\Big) \Delta t \sum_{n=1}^{M} \|\phi_{h,2}^{n}\|_{\Omega_2}^2 \\
&\quad + \kappa^6(\nu_1 + \nu_{T,1})^{-5} S_M \Delta t \sum_{n=1}^{M} \Big(\|\boldsymbol{\phi}_{h,1}^{n-1}\|_{\Omega_1}^2 + \|\boldsymbol{\phi}_{h,2}^{n-1}\|_{\Omega_2}^2\Big).
\end{aligned} \tag{5.39}
$$

Similar to the derivation of (5.39), we can bound the right hand side of (5.8). Combining it with (5.39) and using (4.11) gives

$$
\begin{aligned}
&\|\boldsymbol{\phi}_h^{M+1}\|^2 - \|\boldsymbol{\phi}_h^{1}\|^2 + \sum_{n=1}^{M} \|\boldsymbol{\phi}_h^{n+1} - \boldsymbol{\phi}_h^{n}\|^2 + 2\kappa \Delta t \sum_{n=1}^{M} \int_I |[\mathbf{u}_h^n]| |\boldsymbol{\phi}_h^{n+1}|^2 ds \\
&\quad + \frac{3}{4}(\nu_1 + \nu_{T,1}) \Delta t \sum_{n=1}^{M} \|\nabla \phi_{h,1}^{n+1}\|^2 + \frac{3}{4}(\nu_2 + \nu_{T,2}) \Delta t \sum_{n=1}^{M} \|\nabla \phi_{h,2}^{n+1}\|^2 \\
&\quad + \frac{1}{8}(\nu_1 + \nu_{T,1}) \Delta t \Big(2 \sum_{n=1}^{M} (\|\nabla \boldsymbol{\phi}_{h,1}^{n+1}\|_{\Omega_1}^2 - \|\nabla \boldsymbol{\phi}_{h,1}^{n}\|_{\Omega_1}^2) + \sum_{n=1}^{M} (\|\nabla \boldsymbol{\phi}_{h,1}^{n}\|_{\Omega_1}^2 - \|\nabla \boldsymbol{\phi}_{h,1}^{n-1}\|_{\Omega_1}^2)\Big) \\
&\quad + \frac{1}{8}(\nu_2 + \nu_{T,2}) \Delta t \Big(2 \sum_{n=1}^{M} (\|\nabla \boldsymbol{\phi}_{h,2}^{n+1}\|_{\Omega_2}^2 - \|\nabla \boldsymbol{\phi}_{h,2}^{n}\|_{\Omega_2}^2) + \sum_{n=1}^{M} (\|\nabla \boldsymbol{\phi}_{h,2}^{n}\|_{\Omega_2}^2 - \|\nabla \boldsymbol{\phi}_{h,2}^{n-1}\|_{\Omega_2}^2)\Big) \\
&\leq C(\Delta t^2 + h^{2k} + (\nu_{T,1}{}^2(\nu_1 + \nu_{T,1})^{-1} + \nu_{T,2}{}^2(\nu_2 + \nu_{T,2})^{-1}) H^{2k}) + C\kappa^6((\nu_1 + \nu_{T,2})^{-5} \\
&\quad + (\nu_2 + \nu_{T,2})^{-5})\Big(1 + \|\!|\nabla \mathbf{u}|\!\|_{\infty,\Omega}^4 + \kappa^6(\|[\mathbf{u}]\|_{\infty,I}^6 + \|\!|\boldsymbol{u}|\!\|_{\infty,I}^6 + S_M)\Big) \Delta t \sum_{n=1}^{M} \|\boldsymbol{\phi}_h^{n+1}\|^2 \\
&\quad + C\Big(\kappa^6((\nu_1 + \nu_{T,2})^{-5} + (\nu_2 + \nu_{T,2})^{-5})(\|\!|\boldsymbol{u}|\!\|_{\infty,I}^6 + \|[\mathbf{u}]\|_{\infty,I}^6 + S_M) + \nu_{T,1}^2 h^{-2}\Big) \Delta t \sum_{n=1}^{M} \|\boldsymbol{\phi}_h^{n}\|^2 \\
&\quad + C\kappa^6((\nu_1 + \nu_{T,2})^{-5} + (\nu_2 + \nu_{T,2})^{-5}) S_M \Delta t \sum_{n=1}^{M} \|\boldsymbol{\phi}_h^{n-1}\|^2.
\end{aligned} \tag{5.40}
$$

Dropping the positive term and using discrete Gronwall Lemma 3.3 produce

$$
\begin{aligned}
&\|\boldsymbol{\phi}_h^{M+1}\|^2 + 2\kappa \Delta t \sum_{n=1}^{M} \int_I |[\mathbf{u}_h^n]| |\boldsymbol{\phi}_h^{n+1}|^2 ds \\
&\quad + \frac{3}{4}(\nu_1 + \nu_{T,1}) \Delta t \sum_{n=1}^{M} \|\nabla \phi_{h_1}^{n+1}\|^2 + \frac{3}{4}(\nu_2 + \nu_{T,2}) \Delta t \sum_{n=1}^{M} \|\nabla \phi_{h,2}^{n+1}\|^2 \\
&\quad + \frac{1}{8}(\nu_1 + \nu_{T,1}) \Delta t (2\|\nabla \boldsymbol{\phi}_{h,1}^{M+1}\|_{\Omega_1}^2 + \|\nabla \boldsymbol{\phi}_{h,1}^{M}\|_{\Omega_1}^2) \\
&\quad + \frac{1}{8}(\nu_2 + \nu_{T,2}) \Delta t (2\|\nabla \boldsymbol{\phi}_{h,2}^{M+1}\|_{\Omega_2}^2 + \|\nabla \boldsymbol{\phi}_{h,2}^{M}\|_{\Omega_2}^2) \\
&\leq \|\boldsymbol{\phi}_h^{1}\|^2 + \frac{1}{8}(\nu_1 + \nu_{T,1}) \Delta t (2\|\nabla \boldsymbol{\phi}_{h,1}^{1}\|_{\Omega_1}^2 + \|\nabla \boldsymbol{\phi}_{h,1}^{0}\|_{\Omega_1}^2)
\end{aligned}
$$

$$+\frac{1}{8}(\nu_2+\nu_{T,2})\Delta t(2\|\nabla \boldsymbol{\phi}^1_{h,2}\|^2_{\Omega_2}+\|\nabla \boldsymbol{\phi}^0_{h,2}\|^2_{\Omega_2})$$
$$+C(\Delta t^2+h^{2k}+(\nu_{T,1}{}^2(\nu_1+\nu_{T,1})^{-1}+\nu_{T,2}{}^2(\nu_2+\nu_{T,2})^{-1})H^{2k}). \tag{5.41}$$

Applying triangle inequalities yields the stated result of the theorem. □

Corollary 5.1. *Let* $(\mathbf{u},\mathbf{p})$ *be a solution of (1.1)–(1.6) with regularity assumptions (5.1) and suppose that* (X_i^h, Q_i^h) *for* $i=1,2$ *is given by* (P_2,P_1) *Taylor Hood finite elements and* L_i^H *is given by* P_1 *polynomials,* $\nu_{T,i}=h$ *and* $H=h$*. Assume the velocity data* $\mathbf{u}^0$, $\mathbf{u}^1$ *satisfies*

$$\|\mathbf{u}(t^1)-\mathbf{u}^1\|_X+\|\mathbf{u}(t^0)-\mathbf{u}^0\|_X\le C_1 h$$

for a generic constant C_1 *independent of* Δt *and* h*. Then the error satisfies*

$$\|\mathbf{u}(t^{M+1})-\mathbf{u}^{M+1}\|^2+\frac{3}{4}(\nu_1+\nu_{T,1})\Delta t\sum_{n=1}^{M}\|\nabla(u_1(t^{n+1})-u_{h,1}^{n+1})\|^2$$
$$+\frac{3}{4}(\nu_2+\nu_{T,2})\Delta t\sum_{n=1}^{M}\|\nabla(u_2(t^{n+1})-u_{h,2}^{n+1})\|^2\le C((\Delta t)^2+h^4). \tag{5.42}$$

6. Numerical studies

In this section, we present several numerical experiments which verify the claimed theoretical results for the proposed GA-VMS method, and also demonstrate its advantage over the underlying GA method in the case of low viscosity flows. Numerical studies of GA-VMS method include a comparison with different types of finite element discretizations of fluid–fluid interaction. The first experiment serves as a support for the orders of convergence given by Corollary 5.1. The energy balance is considered in the second experiment. Lastly, we consider the “flow over a cliff” type of problem. The simulations were performed with the Taylor–Hood pair of spaces (P_2,P_1) for velocity and pressure, and also piecewise linear finite element space P_1 for the large scale space on the same mesh instead of piecewise quadratic finite element space P_2 on a different coarse mesh (which would otherwise require transfer of solutions from one mesh to the other, which adds extra computational complexity — see [19]).

We first compare our results with GA of [2]. The scheme reads: Find $(u_{h,i}^{n+1}, p_{h,i}^{n+1})\in(X_i^h,Q_i^h)$ satisfying

$$(\frac{u_{h,i}^{n+1}-u_{h,i}^n}{\Delta t}, v_{h,i})_{\Omega_i}+\nu_i(\nabla u_{h,i}^{n+1},\nabla v_{h,i})_{\Omega_i}+(u_{h,i}^{n+1}\cdot\nabla u_{h,i}^{n+1}, v_{h,i})_{\Omega_i}-(p_{h,i}^{n+1},\nabla\cdot v_{h,i})$$
$$+(\nabla\cdot u_{h,i}^{n+1}, q_{h,i})_{\Omega_i}+\kappa\int_I|[\mathbf{u}_h^n]|u_{h,i}^{n+1}v_{h,i}ds-\kappa\int_I u_{h,j}^n|[\mathbf{u}_h^n]|^{1/2}[\mathbf{u}_h^{n-1}]^{1/2}v_{h,i}ds=(f_i^{n+1},v_{h,i})_{\Omega_i} \tag{6.1}$$

for all $(v_{h,i},q_{h,i})\in(X_i^h,Q_i^h)$.

In addition, we also use monolithically coupled algorithms for comparison. This way, the proposed model could be compared against computationally very expensive, yet highly accurate, in terms of interface coupling, solutions. TWM and TWM-VMS refer to solving the system two-way monolithically and two-way monolithically with variational multiscale method, respectively. Galerkin FEM approximation of TWM method reads: Find $(u_{h,i}^{n+1}, p_{h,i}^{n+1})\in(X_i^h,Q_i^h)$ satisfying

$$(\frac{u_{h,i}^{n+1}-u_{h,i}^n}{\Delta t}, v_{h,i})_{\Omega_i}+\nu_i(\nabla u_{h,i}^{n+1},\nabla v_{h,i})_{\Omega_i}+(u_{h,i}^{n+1}\cdot\nabla u_{h,i}^{n+1}, v_{h,i})_{\Omega_i}-(p_{h,i}^{n+1},\nabla\cdot v_{h,i})$$
$$+(\nabla\cdot u_{h,i}^{n+1}, q_{h,i})_{\Omega_i}+\kappa\int_I|[\mathbf{u}_h^n]|[\mathbf{u}_h^{n+1}]v_{h,i}ds=(f_i^{n+1},v_{h,i})_{\Omega_i}, \tag{6.2}$$

for all $(v_{h,i},q_{h,i})\in(X_i^h,Q_i^h)$. Similar to GA-VMS method, TWM-VMS finite element discretization reads: Find $(u_{h,i}^{n+1}, p_{h,i}^{n+1},\mathbb{G}_i^{\mathbb{H},n+1})\in(X_i^h,Q_i^h,L_i^H)$ satisfying

$$(\frac{u_{h,i}^{n+1}-u_{h,i}^n}{\Delta t}, v_{h,i})_{\Omega_i}+(\nu_i+\nu_{T,i})(\nabla u_{h,i}^{n+1},\nabla v_{h,i})_{\Omega_i}+(u_{h,i}^{n+1}\cdot\nabla u_{h,i}^{n+1}, v_{h,i})_{\Omega_i}-(p_{h,i}^{n+1},\nabla\cdot v_{h,i})$$
$$+(\nabla\cdot u_{h,i}^{n+1}, q_{h,i})_{\Omega_i}+\kappa\int_I|[\mathbf{u}_h^n]|[\mathbf{u}_h^{n+1}]v_{h,i}ds=(f_i^{n+1},v_{h,i})_{\Omega_i}+\nu_{T,i}(\mathbb{G}_i^{\mathbb{H},n},\nabla v_{h,i}), \tag{6.3}$$

Table 1
$\nu_1 = 0.5,\ \nu_2 = 0.1,\ \kappa = 0.001$.

	Errors and rates with GA				Errors and rates with GA-VMS			
$1/h$	$\|\|u-u^h\|\|_{L^2L^2}$	CR	$\|\|u-u^h\|\|_{L^2H^1}$	CR	$\|\|u-u^h\|\|_{L^2L^2}$	CR	$\|\|u-u^h\|\|_{L^2H^1}$	CR
8	1.73449e−04	–	8.24852e−03	–	2.54902e−04	–	8.39643e−03	–
16	3.80466e−05	2.19	2.04670e−03	2.01	4.86909e−05	2.39	2.06158e−03	2.03
32	9.16182e−06	2.05	5.10721e−04	2.00	1.04724e−05	2.22	5.12344e−04	2.01
64	2.26916e−06	2.01	1.27623e−04	2.00	2.42949e−06	2.11	1.27811e−04	2.00

Table 2
$\nu_1 = 0.5,\ \nu_2 = 0.1,\ \kappa = 0.001$.

	Errors and rates with TWM				Errors and rates with TWM-VMS			
$1/h$	$\|\|u-u^h\|\|_{L^2L^2}$	CR	$\|\|u-u^h\|\|_{L^2H^1}$	CR	$\|\|u-u^h\|\|_{L^2L^2}$	CR	$\|\|u-u^h\|\|_{L^2H^1}$	CR
8	1.67933e−04	–	8.23653e−03	–	1.95624e−04	–	8.36568e−03	–
16	3.64680e−05	2.20	2.04372e−03	2.01	4.59099e−05	2.09	2.05606e−03	2.02
32	8.75103e−06	2.06	5.09978e−04	2.00	9.88564e−06	2.21	5.11277e−04	2.01
64	2.16553e−06	2.01	1.27437e−04	2.00	2.30198e−06	2.10	1.27585e−04	2.00

$$(\mathbb{G}_i^{\mathbb{H},n} - \nabla u_{h,i}^n, \mathbb{L}_i^H)_{\Omega_i} = 0, \tag{6.4}$$

for all $(v_{h,i}, q_{h,i}, \mathbb{L}_i^H) \in (X_i^h, Q_i^h, L_i^H)$.

Simulations were performed at a problem defined in $\Omega = \Omega_1 \cup \Omega_2$ with $\Omega_1 = [0,1] \times [0,1]$ and $\Omega_2 = [0,1] \times [0,-1]$ with prescribed solution

$$\begin{aligned}
u_{1,1} &= a\nu_1 e^{-2bt} x^2(1-x)^2(1+y) + ae^{-bt}x(1-x)\nu_1/\sqrt{\kappa a}\\
u_{1,2} &= a\nu_1 e^{-2bt} xy(2+y)(1-x)(2x-1) + ae^{-bt}y(2x-1)\nu_1/\sqrt{\kappa a}\\
u_{2,1} &= a\nu_1 e^{-2bt} x^2(1-x)^2(1+\frac{\nu_1}{\nu_2}y)\\
u_{2,2} &= a\nu_1 e^{-2bt} xy(1-x)(2x-1)(2+\frac{\nu_1}{\nu_2}y),
\end{aligned}$$

Herein, for simplicity pressures are set to zero in both domains, and right hand side forcing, boundary and two initial values are computed using the manufactured true solution as is done in [4]. Problem parameters, $a = 1$, $b = 1/2$ and the final time $T = 1$ are fixed while κ, ν_1 and ν_2 vary from one computation to the other. Numerical experiments are performed on a single mesh, that is $H = h$. Also discretization parameters, h, $\Delta t = h^2$ and the eddy viscosity parameter $\nu_{T,1} = \nu_{T,2} = h$ are refined all together. Therefore, second order accuracy is expected in numerical experiments.

Convergence Rates. Results with the high viscosity and weak coupling are presented in Tables 1–2. These results agree with the analytical predictions in terms of accuracy. This serves as a verification of GA's effectiveness in decoupling the laminar fluid–fluid interaction problems. Another computation has been performed with low viscosity in the lower domain and stronger coupling on the interface. It is observed that GA and TWM both fail to converge, unless the discretization parameters have been substantially refined. Even as the mesh diameter and the time step have been refined and GA and TWM start converging, their accuracy is much worse, than that of the GA-VMS — which validates the necessity of incorporating a turbulence model, as in GA-VMS. Consequently, equipping GA and TWM with VMS regularizes their systems and produces believable results for this setting, see Tables 3–4 for the choices $\nu_1 = 0.1$, $\nu_2 = 0.0001$, $\kappa = 1$. Altogether, the behavior of the discrete solutions observed here is in agreement with the analytical results: GA-VMS is a second order in space and first order in time accuracy model of fluid–fluid interaction. It can be also observed that decoupling systems will not introduce too much error as TWM-VMS and GA-VMS both give very similar accuracy results. This might be attributed to the viscosity error dominating the decoupling error.

To save horizontal space in the following tables, let the error norms $\| u - u^h \|_{L^2(0,T;L^2(\Omega))}$ and $\| u - u^h \|_{L^2(0,T;H^1(\Omega))}$ be abbreviated to $\|u - u^h\|_{L^2L^2}$ and $\|u - u^h\|_{L^2H^1}$, respectively.

Table 3
$\nu_1 = 0.1,\ \nu_2 = 0.0001,\ \kappa = 1.$

	Errors and rates with GA				Errors and rates with GA-VMS			
$1/h$	$\|\|u-u^h\|\|_{L^2L^2}$	CR	$\|\|u-u^h\|\|_{L^2H^1}$	CR	$\|\|u-u^h\|\|_{L^2L^2}$	CR	$\|\|u-u^h\|\|_{L^2H^1}$	CR
8	not conv.	–	not conv.	–	1.93634e−02	–	4.69936e−01	–
16	not conv.	–	not conv.	–	2.97186e−03	2.70	1.28426e−01	1.87
32	not conv.	–	not conv.	–	3.21593e−04	3.21	2.81163e−02	2.19
64	3.99034e−04	–	1.47302e−01	–	3.77500e−05	3.09	6.22355e−03	2.18

Table 4
$\nu_1 = 0.1,\ \nu_2 = 0.0001,\ \kappa = 1.$

	Errors and rates with TWM				Errors and rates with TWM-VMS			
$1/h$	$\|\|u-u^h\|\|_{L^2L^2}$	CR	$\|\|u-u^h\|\|_{L^2H^1}$	CR	$\|\|u-u^h\|\|_{L^2L^2}$	CR	$\|\|u-u^h\|\|_{L^2H^1}$	CR
8	not conv.	–	not conv.	–	1.cma11299093652e−02	–	4.69974e−01	–
16	not conv.	–	not conv.	–	2.87967e−03	2.75	1.28333e−01	1.87
32	not conv.	–	not conv.	–	3.21353e−04	3.16	2.80955e−02	2.19
64	3.99033e−04	–	1.47302e−01	–	3.77021e−05	3.09	6.22028e−03	2.18

Table 5
GA-VMS alternative approach for $\nu_1 = 0.5,\ \nu_2 = 0.1,\ \kappa = 0.001.$

$1/h$	$\|\|u-u^h\|\|_{L^2L^2}$	Rate	$\|\|u-u^h\|\|_{L^2H^1}$	Rate
8	2.69576e−03	–	2.82051e−02	–
16	1.30156e−03	1.05	1.33436e−02	1.08
32	6.42476e−04	1.02	6.55157e−03	1.03
64	3.20172e−04	1.00	3.25761e−03	1.01

It has to be noted that the alternative approach for GA-VMS mentioned on Remark 2.2 fails to provide good-quality results, see Table 5.

Conservation of Energy. Computational results related to conservation of global energy are presented next. For simplicity, the problem has been set to keep the same total energy over all time levels. For this reason, we choose homogeneous Dirichlet boundary conditions everywhere except the interface, and choose zero forcing. Expectations of the energy have to be discussed before presenting any computational results. To that end, weak formulation of the continuous problem shall be considered under homogeneous boundary conditions and zero forcing: Multiplying (1.1) by $\mathbf{u} \in X$, integrating over the whole domain and over $[0, T]$, we get the following energy equality:

$$\|\mathbf{u}(T)\|^2_{\Omega} + 2\nu_1 \int_0^T \|\nabla u_1(t)\|^2_{\Omega_1} dt + 2\nu_2 \int_0^T \|\nabla u_2(t)\|^2_{\Omega_2} dt + 2\kappa \int_0^T \int_I |[\mathbf{u}(t)]|^3 ds dt = \|\mathbf{u}(0)\|^2_{\Omega}. \tag{6.5}$$

Herein, define

$$\begin{aligned}
I &:= \text{initial kinetic energy} &&= \|\mathbf{u}(0)\|^2_{\Omega} = \|u_1(0)\|^2_{\Omega_1} + \|u_2(0)\|^2_{\Omega_2},\\
KE &:= \text{kinetic energy at T} &&= \|\mathbf{u}(T)\|^2_{\Omega} = \|u_1(T)\|^2_{\Omega_1} + \|u_2(T)\|^2_{\Omega_2},\\
\mathcal{E} &:= \text{energy dissipated by the time T} &&= 2\nu_1 \int_0^T \|\nabla u_1(T)\|^2_{\Omega_1} dt\\
& &&\quad + 2\nu_2 \int_0^T \|\nabla u_2(T)\|^2_{\Omega_2} dt.\\
\mathcal{E}_I &:= \text{ interface dissipation by the time T} &&= 2\kappa \int_0^T \int_I |[\mathbf{u}(t)]|^3 ds dt\\
& &&= 2\kappa \int_0^T \int_I |[\mathbf{u}(t)]|[\mathbf{u}(t)] u_1(t) ds dt\\
& &&\quad - 2\kappa \int_0^T \int_I |[\mathbf{u}(t)]|[\mathbf{u}(t)] u_2(t) ds dt
\end{aligned}$$

Energy equality (6.5) means continuous system conserves global energy for all time. However, discrete models introduce discretization errors such as decoupling errors, consequently, energy is not exactly conserved. On the other hand, both GA and GA-VMS have their own exact energy conservation properties, see Eq. (4.1) and Lemma 3.1 in [2].

The following quantity gives a measurement of how far away energy goes beyond being exact. Considering (6.7), we define

$$AED_h^M := \text{absolute energy difference at } T(=t_{M+1}) = |I^1 - KE^{M+1} - \mathcal{E}^{M+1}|. \tag{6.6}$$

$$\begin{aligned}
I^1 &= \|u_{h,1}^1\|_{\Omega_1}^2 + \|u_{h,2}^1\|_{\Omega_2}^2 + \Delta t\big(\nu_{T,1}\|\nabla u_{h,1}^1\|_{\Omega_1}^2 + \nu_{T,2}\|\nabla u_{h,2}^1\|_{\Omega_2}^2\big) + \kappa\Delta t\int_I |[u_h^0]|(|u_{h,1}^1|^2 + |u_{h,2}^1|^2)ds,\\
KE^{M+1} &= \|u_{h,1}^{M+1}\|_{\Omega_1}^2 + \|u_{h,2}^{M+1}\|_{\Omega_2}^2 + \kappa\Delta t\int_I |[\mathbf{u}_h^M]|(|u_{h,1}^{M+1}|^2 + |u_{h,2}^{M+1}|^2)ds\\
&+ \Delta t\sum_{n=1}^{M}(\|u_{h,1}^{n+1} - u_{h,1}^n\|_{\Omega_1}^2 + \|u_{h,2}^{n+1} - u_{h,2}^n\|_{\Omega_2}^2),\\
\mathcal{E}^{M+1} &= \Delta t\big(\nu_{T,1}\|\nabla u_{h,1}^{M+1}\|_{\Omega_1}^2 + \nu_{T,2}\|\nabla u_{h,2}^{M+1}\|_{\Omega_2}^2\big)\\
&+ \Delta t\sum_{n=1}^{M}\Big(2\nu_1\|\nabla u_{h,1}^{n+1}\|_{\Omega_1}^2 + \nu_{T,1}\|\nabla u_{h,1}^{n+1} - \mathbb{G}_1^{\mathbb{H},n}\|_{\Omega_1}^2 + \nu_{T,1}\|\nabla u_{h,1}^n - \mathbb{G}_1^{\mathbb{H},n}\|_{\Omega_1}^2\Big)\\
&+ \Delta t\sum_{n=1}^{M}\Big(2\nu_2\|\nabla u_{h,2}^{n+1}\|_{\Omega_2}^2 + \nu_{T,2}\|\nabla u_{h,2}^{n+1} - \mathbb{G}_2^{\mathbb{H},n}\|_{\Omega_2}^2 + \nu_{T,2}\|\nabla u_{h,2}^n - \mathbb{G}_2^{\mathbb{H},n}\|_{\Omega_2}^2\Big)\\
&+ \kappa\Delta t\sum_{n=1}^{M}\int_I \Big||[\mathbf{u}_h^n]|^{1/2}u_{h,1}^{n+1} - |[\mathbf{u}_h^{n-1}]|^{1/2}u_{h,2}^n\Big|^2 ds + \kappa\Delta t\sum_{n=1}^{M}\int_I \Big||[\mathbf{u}_h^n]|^{1/2}u_{h,2}^{n+1} - |[\mathbf{u}_h^{n-1}]|^{1/2}u_{h,1}^n\Big|^2 ds.
\end{aligned} \tag{6.7}$$

As mentioned above for continuous solution, the problem has been constructed so that it has zero forcing and homogeneous Dirichlet boundary conditions everywhere except the interface, and divergence-free initial values, $u_{i,j}^0$ have been chosen as follows:

$$\begin{aligned}
u_{i,1} &= \sin(2\pi y)\sin^2(\pi x),\\
u_{i,2} &= -\sin(2\pi x)\sin^2(\pi y),\ i = 1, 2.
\end{aligned} \tag{6.8}$$

Both GA and GA-VMS require two initial values. Therefore, we compute the second initial values with one step of IMEX method proposed in [2] and investigated in [3].

Discretization parameters are chosen uniform, $h = 1/32$, $\Delta t = 0.01$, and computations ended at the final time $T = 25$. $\kappa = 1000$ is chosen fixed and code has been run twice: one with high and the other with small ν_1 and ν_2 values. All computations have been performed on the uniform square mesh shown faded in Fig. 1. Noting the fact that global energy is exactly conserved in the true solution of fluid–fluid interaction, any proposed model shall conserve it as much as possible. The absolute differences between the total energy and the initial energy input are computed over all the time levels, and presented in Fig. 2. Both GA and GA-VMS perform equally well when applied to a fluid–fluid interaction problem at high viscosity. However, Fig. 2 illustrates that, when viscosities are low, the GA solution blows up around $t = 4.5$ while GA-VMS conserves global energy all the time.

Long-Time Stability. We now present computational results for the long-time stability of GA and GA-VMS. This is investigated for a problem, where a parabolic inflow in the atmosphere passes a backward-facing step — a widely used benchmark problem for one-domain fluid-flow — before atmosphere and ocean meet, see the domain in Fig. 3. Note that this setup could be a description of a coast mountain, cliff, etc. in a real life simulation.

Homogeneous Dirichlet boundary conditions have been strongly enforced on the step, on the left wall and the bottom of the ocean. While parabolic inflow profile with maximum inlet 1 drives the flow in the atmosphere,“do nothing” boundary conditions are weakly imposed on the outflow, on the top of atmosphere and the right wall of the ocean. Both fluids are at rest initially, and the second initial values have been computed by one-step of IMEX

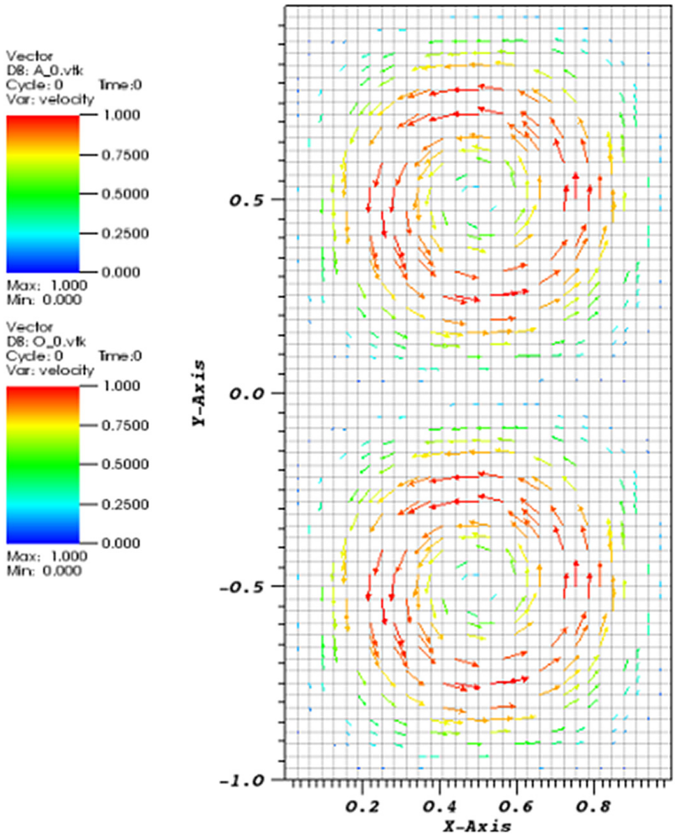

Fig. 1. Initial flows.

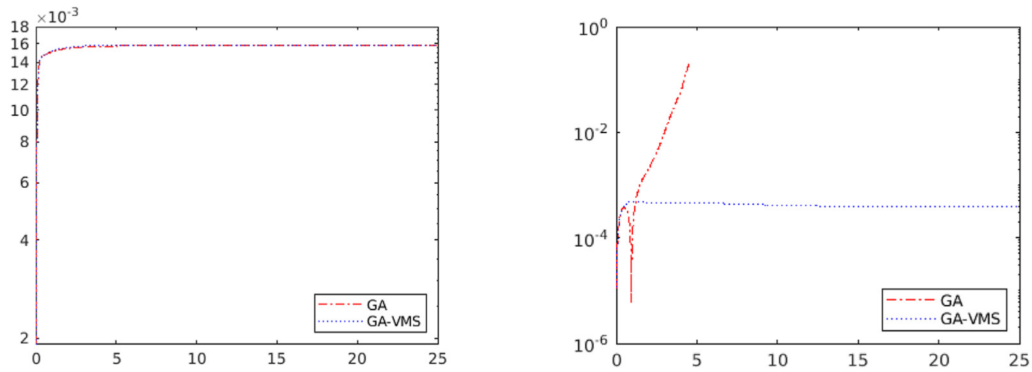

Fig. 2. AED_h^M for $\nu_1 = 1.5e-01$, $\nu_2 = 1.0e-02$ on the left and for $\nu_1 = 1.5e-05$, $\nu_2 = 1.0e-06$ on the right.

method as in the previous example, i.e. flows in both domains start with the same initial values. The rest of the parameters have been chosen as in Table 6.

Fig. 4 illustrates that the GA solution starts blowing up around $t = 25$, while GA-VMS produces stable results all the way up to final time $T = 100$.

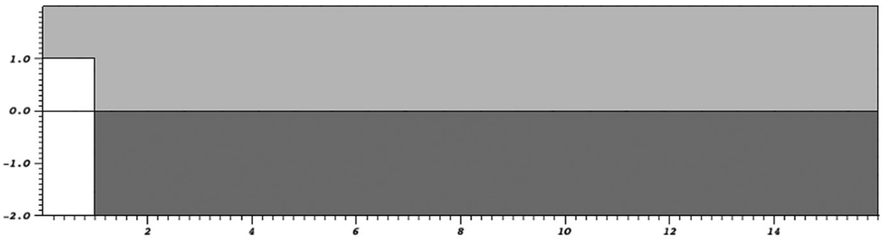

Fig. 3. Domain.

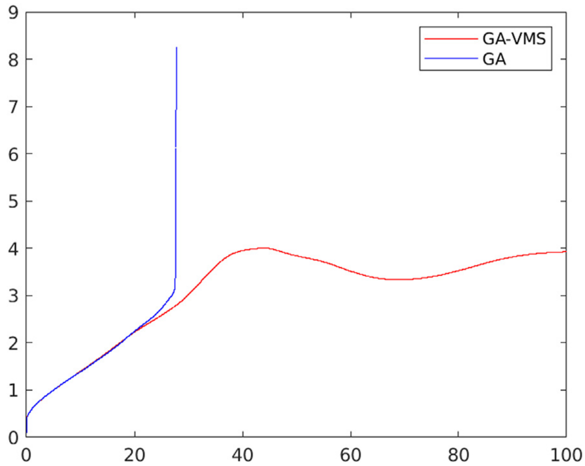

Fig. 4. Temporal evolution of $\|u_h^{n+1}\|$ with GA and GA-VMS.

Table 6
Problem parameters.

ν_1	ν_2	κ	T	Δt	h	$\nu_{T,1} = \nu_{T,2}$
5e−04	5e−03	2.45e−03	100	0.01	0.1–0.14	0.01

Table 7
Computational times.

GA	33 m:16 s
GA-VMS	23 m:35 s

Expected vector fields with GA and GA-VMS (in Fig. 5) illustrate that both methods produce very similar results as long as they are both stable. However, as seen in Figs. 5(e) and 5(g), solution with GA has already started blowing up around $t = 25$.

In addition to checking long time stability properties of methods, computational times have been recorded up to $t = 20$. This time has been chosen in particular so that GA does not yet start to blow up and both methods still produce similar results. It is observed that it takes much longer time for GA to converge, as seen in Table 7. Also, it has to be noted that this computation has still been performed on a regime where GA produces reliable results up to some time, changing parameters to increase the numerical singularity has a greater impact on computational time than reported here.

Figs. 5 and 6 suggest that the interface flow in the ocean tends to follow the direction of the flow just above. For this reason, all consistent direction changes on the interface of the atmosphere results in a separate vortex formation right below. Furthermore, the reattachment point in the atmospheric flow and the separation point of two vertices

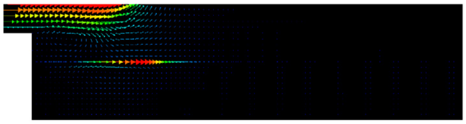

(a) GA at t=10

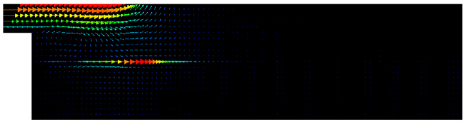

(b) GA-VMS at t=10

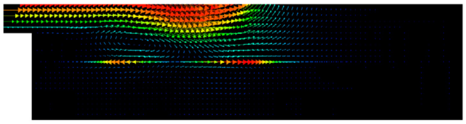

(c) GA at t=20

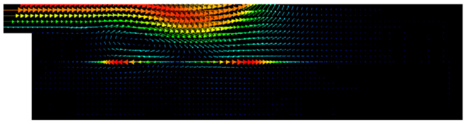

(d) GA-VMS at t=20

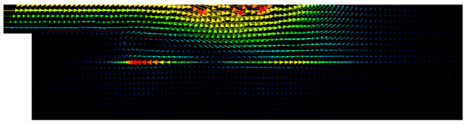

(e) GA at t=25

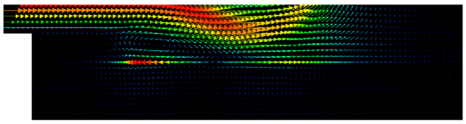

(f) GA-VMS at t=25

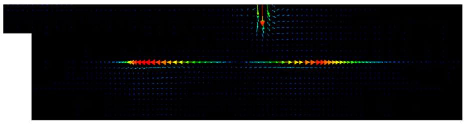

(g) GA at t=27.75

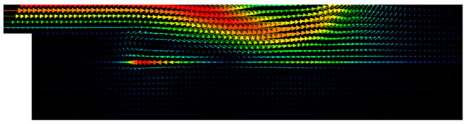

(h) GA-VMS at t=27.75

Fig. 5. Expected vector fields with GA and GA-VMS.

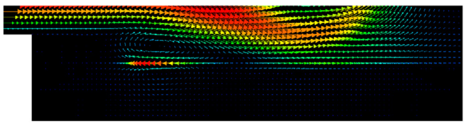

(a) GA-VMS at t=30

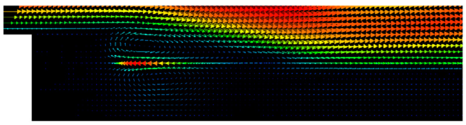

(b) GA-VMS at t=40

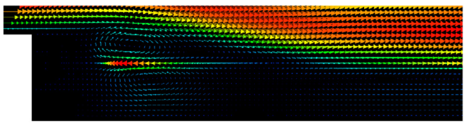

(c) GA-VMS at t=50

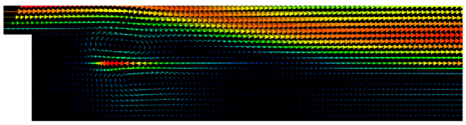

(d) GA-VMS at t=60

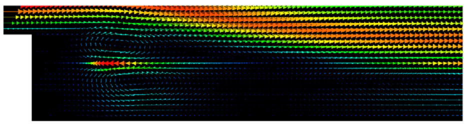

(e) GA-VMS at t=70

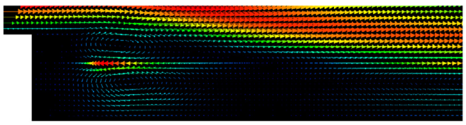

(f) GA-VMS at t=80

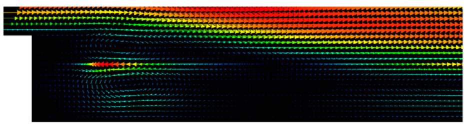

(g) GA-VMS at t=90

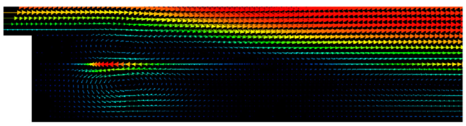

(h) GA-VMS at t=100

Fig. 6. Expected vector fields with GA-VMS.

in the ocean coincide. One can intuitively expect this phenomenon already since, for this setting, the oceanic flow is due to merely its interaction with the atmosphere and possess of very low energy to determine its own persistent direction.

7. Conclusions

In this report we introduced a method for approximating solutions to a turbulent fluid–fluid interaction problem (1.1)–(1.6). The method combines the Geometric Averaging method for stable decoupling of the two-domain problem with the Variational Multiscale stabilization technique for high Reynolds number flows. We performed full numerical analysis of the method, proving its stability and accuracy. One of the challenges we had to overcome was the lack of benchmark problems for qualitative testing of our method in the case of low viscosities, $\nu \ll 1$. In addition to verifying numerically the claimed theoretical accuracy of the method in the case of a known true solution, we also used two other numerical tests to assess the qualitative behavior of the solution. First, we showed that the total global energy of the approximate solution is better conserved with the proposed method — as it should be in the continuous coupled solution. Secondly, we introduced a "flow over a cliff" type of a problem, which could serve as an analogue of flow over a step, in the case of fluid–fluid interaction. The vortices forming and detaching in the air domain were closely matched by the sea regions with increased flow velocity. The GA method (without the VMS component) had failed to work in any of the tests, if the viscosity coefficient was taken to be small enough, while the proposed GA-VMS technique has matched the expectations both quantitatively and qualitatively.

Declaration of competing interest

The authors declare that they have no known competing financial interests or personal relationships that could have appeared to influence the work reported in this paper.

References

[1] D. Bresch, J. Koko, Operator-splitting and Lagrange multiplier domain decomposition methods for numerical simulation of two coupled Navier-Stokes, Int. J. Appl. Math. Comput. Sci. 16 (2006) 419–429.
[2] J. Connors, J. Howell, W. Layton, Decoupled time stepping methods for fluid-fluid interaction, SIAM J. Numer. Anal. 50(3) (2012) 1297–1319.
[3] Y. Zhang, Y. Hou, L. Shano, Stability and convergence analysis of a decoupled algorithm for a fluid-fluid interaction problem, SIAM J. Numer. Anal. 54(5) (2016) 2833–2867.
[4] M. Aggul, J. Connors, D. Erkmen, A. Labovsky, A defect-deferred correction method for fluid-fluid interaction, SIAM J. Numer. Anal. 56 (2018) 2484–2512.
[5] J.-L. Lions, R. Temam, S. Wang, Models of the coupled atmosphere and ocean (CAO I), Comput. Mech. Adv. 1 (1993) 5–54.
[6] J.-L. Lions, R. Temam, S. Wang, Numerical analysis of the coupled atmosphere and ocean models (CAO II), Comput. Mech. Adv. 1 (1993) 55–120.
[7] J.-W. Bao, J.M. Wilczak, J.-K. Choi, L.H. Kantha, Numerical simulations of air-sea interaction under high wind conditions using a coupled model: A study of hurricane development, Mon. Weather Rev. 128 (2000) 2190–2210.
[8] F.O. Bryan, B.G. Kauffman, W.G. Large, P.R. Gent, The NCAR CSM flux coupler, Tech. Report NCAR/TN-424+STR, National Center for Atmosphere Research, 1996.
[9] N. Perlin, E.D. Skyllingstad, R.M. Samelson, P.L. Barbour, Numerical simulation of air-sea coupling during coastal upwelling, J. Phys. Oceanogr. 37 (2007) 2081–2093.
[10] J. Connors, B. Ganis, Stability of algorithms for a two domain natural convection problem and observed model uncertainty, Comput. Geosci. 15 (2011) 509–527.
[11] F. Lemarié, E. Blayo, L. Debreu, Analysis of ocean-atmosphere coupling algorithms: consistency and stability, Procedia Comput. Sci. 51 (2015) 2066–2075.
[12] M. Marion, J. Xu, Error estimates for a new nonlinear Galerkin method based on two-grid finite elements, SIAM J. Numer. Anal. 32 (1995) 1170–1184.
[13] V. Girault, J.-L. Lions, Two-grid finite-element schemes for the steady Navier-Stokes problem in polyhedra, Port. Math. 58 (2001) 25–57.
[14] V. Girault, J.-L. Lions, Two-grid finite-element schemes for the transient Navier-Stokes problem, Math. Model. Numer. Anal. 35 (2001) 945–980.
[15] T.J.R. Hughes, Multiscale phenomena: Green's functions, the Dirichlet-to-Neumann formulation, subgrid-scale models, bubbles and the origins of stabilized methods, Comput. Methods Appl. Mech. Engrg. 127 (1995) 387–401.
[16] J.-L. Guermond, Stabilization of Galerkin approximations of transport equations by subgrid modeling, Math. Model. Numer. Anal. 33 (1999) 1293–1316.

[17] V. Gravemeier, W.A. Wall, E. Ramm, A three-level finite element method for the instationary incompressible Navier–Stokes equations, Comput. Methods Appl. Mech. Engrg. 193 (2004) 1323–1366.
[18] S. Ramakrishnan, S.S. Collis, Multiscale modeling for turbulence simulation in complex geometries, AIAA Paper 2004-0241, 2004.
[19] V. John, S. Kaya, A finite element variational multiscale method for the Navier-Stokes equations, SIAM J. Sci. Comput. 26 (2005) 1485–1503.
[20] V. John, S. Kaya, W. Layton, A two-level variational multiscale method for convection-dominated convection-diffusion equations, Comput. Methods Appl. Mech. Engrg. 195 (2006) 4594–4603.
[21] W. Layton, A connection between subgrid scale eddy viscosity and mixed methods, Appl. Math. Comput. 133 (2002) 147–157.
[22] N. Ahmed, T.C. Rebollo, V. John, S. Rubino, A review of variational multiscale methods for the simulation of turbulent incompressible flows, Arch. Comput. Methods Eng. 24 (2017) 115–164.
[23] V. Girault, P.A. Raviart, Finite Element Approximation of the Navier-Stokes Equations, in: Lecture Notes in Math., vol. 749, Springer-Verlag, Berlin, 1979.
[24] M. Gunzburger, Finite Element Methods for Viscous Incompressible Flow: A Guide to Theory, Practice, and Algorithms, Academic Press, Boston, 1989.
[25] V. John, A. Kindl, Variants of projection-based finite element variational multiscale methods for the simulation of turbulent flows, Internat. J. Numer. Methods Fluids 56 (2008) 1321–1328.
[26] V. John, A. Kindl, Numerical studies of finite element variational multiscale methods for turbulent flow simulations., Comput. Methods Appl. Mech. Engrg. 199 (2010) 841–852.
[27] G.P. Galdi, An Introduction to the Mathematical Theory of the Navier-Stokes Equations, Volume I, Springer-Verlag, New York, 1994.
[28] J. Heywood, R. Rannacher, Finite element approximation of the nonstationary Navier-Stokes equations, part II: Stability of solutions and error estimates uniform in time, SIAM J. Numer. Anal. 23 (1986) 750–777.